1-1-2018

Study of Optical OFDM System for Wireless LAN Applications

Salih Mohamed S. Kenshil
University of Denver

Study of Optical OFDM System for Wireless LAN Applications

Abstract

The advantages of optical fiber make it possible to extend the data rate transmission and propagation distance. Orthogonal frequency division multiplexing (OFDM) as a multicarrier technique (MC) is used in hybrid optical-wireless system designs because it has the best spectral efficiency to radio frequency (RF) interference and lower multipath distortion. In this dissertation, a study and evaluation of optical OFDM based wireless local area network (W-LAN) systems are presented. The baseband of the OFDM signal is fully transmitted and up-converted to a radio frequency signal. Also, to reduce system costs, simple base stations (BSs) are interconnected to a central office (CO) via an optical fiber. All the required operations are achieved in the CO. The directly modulated laser (DML) and continuous wave (CW) laser are used in the system simulations as optical laser sources. Identical rectangular microstrip patch antennas have been used at the transmitter and the receiver as well. The simulations were carried out for different SMF and MMF lengths, and the variable wireless distance between the transmitting and receiving antennas was in a range of 40 dB to 80 dB.

The purpose of this work is to provide a framework for integrating wireless and optical technologies in one system with the presence of OFDM technology. The required microstrip patch antenna parameters for the system are analyzed and designed. The microstrip patch antenna (S-parameters) is loaded into the Optisystem communication software tool in *Touchstone format*. As a result, this achievement gives a greater impetus to design an integrated optical-wireless system, and simulation results validate the proposed technique.

Then, the integration of the microstrip patch antenna and optical OFDM system is achieved, and the performance is intensely studied. The entire system has been presented by developing analytical models and simulations.

The system performance results are obtained regarding EIRP, SNR, signal constellations and BER. The results show that this integrated optical wireless link is very robust for carrying OFDM based wireless LAN signals over an optical fiber. Moreover, using an active patch antenna in the system helps to increase the coverage service to more than 30 meters when an SMF of 80 km length is utilized.

Document Type

Dissertation

Degree Name

Ph.D.

Department

Electrical Engineering

First Advisor

Mohammad Matin, Ph.D.

Second Advisor

Vijaya Narapareddy, Ph.D.

Third Advisor

Ronald DeLyser

STUDY OF OPTICAL OFDM SYSTEM FOR WIRELESS LAN APPLICATIONS

_____

A Dissertation

Presented to

the Faculty of the Daniel Felix Ritchie School of Engineering and Computer Science

University of Denver

_____

In Partial Fulfillment

of the Requirements for the Degree

Doctor of Philosophy

_____

by

Salih Mohamed S. Kenshil

June 2018

Advisor: Mohammad Matin

Author: Salih Mohamed S. Kenshil
Title: **STUDY OF OPTICAL OFDM SYSTEM FOR WIRELESS LAN APPLICATIONS**
Advisor: Mohammad Matin
Degree Date: June 2018

Abstract

The advantages of optical fiber make it possible to extend the data rate transmission and propagation distance. Orthogonal frequency division multiplexing (OFDM) as a multicarrier technique (MC) is used in hybrid optical-wireless system designs because it has the best spectral efficiency to radio frequency (RF) interference and lower multipath distortion. In this dissertation, a study and evaluation of optical OFDM based wireless local area network (W-LAN) systems are presented. The baseband of the OFDM signal is fully transmitted and up-converted to a radio frequency signal. Also, to reduce system costs, simple base stations (BSs) are interconnected to a central office (CO) via an optical fiber. All the required operations are achieved in the CO. The directly modulated laser (DML) and continuous wave (CW) laser are used in the system simulations as optical laser sources. Identical rectangular microstrip patch antennas have been used at the transmitter and the receiver as well. The simulations were carried out for different SMF and MMF lengths, and the variable wireless distance between the transmitting and receiving antennas was in a range of 40 dB to 80 dB.

The purpose of this work is to provide a framework for integrating wireless and optical technologies in one system with the presence of OFDM technology. The required microstrip patch antenna parameters for the system are analyzed and designed. The microstrip patch antenna (S-parameters) is loaded into the Optisystem communication software tool in *Touchstone format*. As a result, this achievement gives a greater impetus

to design an integrated optical-wireless system, and simulation results validate the proposed technique.

Then, the integration of the microstrip patch antenna and optical OFDM system is achieved, and the performance is intensely studied. The entire system has been presented by developing analytical models and simulations.

The system performance results are obtained regarding EIRP, SNR, signal constellations and BER. The results show that this integrated optical wireless link is very robust for carrying OFDM based wireless LAN signals over an optical fiber. Moreover, using an active patch antenna in the system helps to increase the coverage service to more than 30 meters when an SMF of 80 km length is utilized.

Acknowledgements

First and foremost, my many thanks to Allah for all his blessings. It is my pleasure to express my most sincere gratitude and appreciation to my advisor, Professor Mohammad Matin, for his fruitful guidance, support, and encouragement. I would also like to express my sincere thanks and gratitude to my family for their unlimited support and patience during my study. Also, my sincere thanks go to my Ph.D. committee members; Professor Ronald DyLaser and Dr. David Gao for their time, support and kindness. I am happy to acknowledge the support of the Department of Electrical and Computer Engineering, the Daniel Felix Ritchie School of Engineering and Computer Science, and the University of Denver for giving me the chance to finish my Ph.D. research.

Table of Contents

List of Figures

List of Tables

List of Abbreviations

ADC:	Analog-to-digital converter
APD:	Avalanche photodiode
BER:	Bit error rate
BSs:	Base stations
CD:	Chromatic dispersion
CFO:	Carrier frequency offset
CO:	Central office
CO-OFDM:	Coherent optical OFDM
CP:	Cyclic prefix
CS:	Central station
CST-MW:	Computer simulation technology Microwave studio
CW:	Continuous wave
DAC:	Digital to analog converter
DCFs:	Dispersion compensating fibers
DD-OOFDM:	Direct-detection optical OFDM
DFB:	Distributed feedback
DFT:	Discrete Fourier transform
DML:	Directly modulated laser
EDFA:	Erbium-doped fiber amplifier
EIRP:	Equivalent isotopically radiated power
FCC:	Federal communications commission
FDM:	Frequency division multiplexing
FFT:	Fast Fourier transform
FPL:	Fabry-Perot laser
FSL:	Free space loss
FSPL:	Free space path loss
GSM:	Global system for mobile
ICI:	Intercarrier interference
IFFT:	Inverse fast Fourier transform

ISI:	Inter-symbol interference
ISM:	Industrial, scientific and medical
LAN:	Local area network
LD:	Laser diode
LED:	Light-emitting diode
LiNb. MZM:	Lithium Niobate MZM
LOS:	Line of Sight
LTE:	Long-term evolution
MB-OFDM:	Multiband-orthogonal frequency division multiplexing technique
MC:	Multicarrier technique
MMF:	Multimode fiber
MSM:	Metal–semiconductor–metal
MZM:	Mach-Zehnder modulator
NF:	Noise figure
OFDM:	Orthogonal frequency division multiplexing
OFDM-UWB:	Orthogonal frequency division multiplexing-ultra-wideband
OIP3:	3rd order output intercept point
OSNR:	Optical signal-to-noise ratio
PAPR:	Peak-to-average power ratio
PRBS:	Pseudo-random bit sequence generator
PTS:	Partial transmit sequences
QAM:	Quadrature amplitude modulation
QD:	Quadrature modulator
QDem:	Quadrature modulator
RF:	Radio frequency
ROF:	Radio over fiber
S2P:	Two-port S-Parameter
SCM:	Single carrier modulation
SLM:	Selective mapping
SMF:	Single mode fiber

SNR:	Signa-to-noise ratio
SOA:	Semiconductor optical amplifiers
S-Parameters:	Scattering parameters
STO:	Symbol time offset
TDMA:	Time division multiple access
TFC:	Time-frequency coding
TFI:	Time-frequency interleaving
TI:	Tone injection
TR:	Tone reservation
UWB:	Ultra-wideband
VCSEL:	Vertical-cavity surface-emitting laser
Wi-Fi:	Wireless fidelity
WiMAX:	Worldwide interoperability for microwave access
W-LAN:	Wireless local area network
WMANs:	Metropolitan area networks
WPANs:	Wireless personal area networks

Chapter One: Introduction

1.1 Background

Due to increasing requirements for high data-rates in modern communication systems, orthogonal frequency division multiplexing (OFDM) has been intensively studied over the last two decades [1-6]. OFDM as a modulation mechanism provides a high data-rate with robustness against a multipath fading channel. The baseband data in OFDM are distributed among several carriers, making the data symbol long enough to overcome any delay spread that the signal may encounter [2], [3]. Moreover, the OFDM technique is widely used in wired and wireless communications because of its poplar advantages for reducing interference and multipath issues compared with conventional single carrier modulation (SCM) techniques [1]. OFDM is applied to different wireless applications; such as wireless fidelity (Wi-Fi) and wireless local area networks (W-LANs) [4]. The unique feature of the OFDM technique is the use of orthogonality between the individual subcarriers. Furthermore, the importance of OFDM is that it has the best spectral efficiency to RF interference and lower multipath distortion [6]. OFDM also adds another advantage that transfers the transceiver complexity from analog to the digital domain [1], [5].

There is a huge demand for supporting some areas with mobile and internet services that are hard to reach with conventional wireless communication links, as in large buildings, shopping malls, and tunnels. However, the distribution of W-LAN

signals according to the IEEE 802.11 standard is an appealing application for indoor and outdoor systems. In the last decade, OFDM has also been implemented in optical communications to overcome wireless coverage area deficiencies [7]. Due to the cost sensitivity of the optical access network, it is necessary to utilize low-cost optical front-ends [8]. 2.4 (GHz) is called the industrial, scientific and medical (ISM) radio band. Operating some technologies at this unlicensed band can offer distance benefits over high frequencies and can also be cheaper compared to using higher frequency bands.

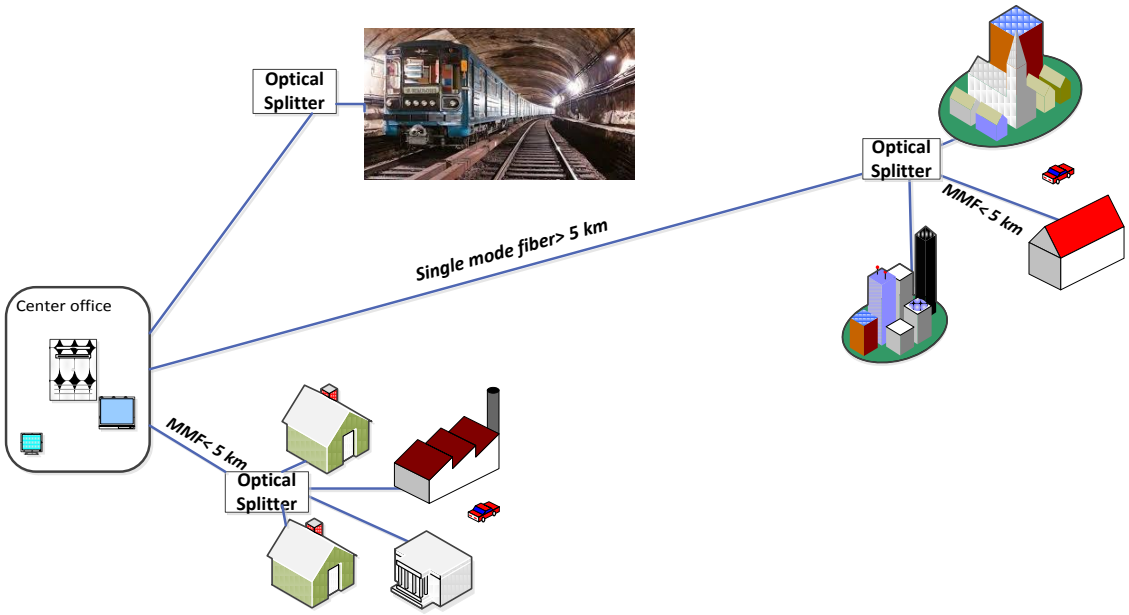

Figure 1.1 Optical OFDM for different scenarios applications

Figure 1.1 shows the proposed applications of an optical OFDM based W-LAN system to certain areas of demand. This system can serve different areas with wireless signals that are hard to reach with conventional wireless communication links, as in large

buildings, shopping malls, and tunnels. The signal is processed at the central office (CO), up-converted and carried over an SMF or MMF, then at the destination distributed wirelessly using a microstrip patch antenna. However, to reduce system costs, simple base stations (BSs) are interconnected to a CO via an optical fiber. All the required operations are achieved in the CO or at the central station (CS).

Identical rectangular microstrip patch antennas are used at the transmitter and the receiver sides. In this study, simulations were carried out for different SMF and MMF fiber lengths up to 80 km and 5 km, respectively, as well as at different wireless propagation distances between the transmitting and receiving antennas, which were in a range of 40 dB to 80 dB.

1.2 Problem Statement

Single carrier modulations (SCMs), such as the global system for mobile (GSM) or time division multiple access (TDMA), have a symbol duration which decreases with increases in the data rate. The multipath fading of the wireless channel causes more severe inter-symbol interference (ISI). Hence, OFDM is used in modern wireless applications, such as a W-LAN, to combat ISI by dividing the entire channel into many narrowband sub-channels that are transmitted in parallel to achieve high data rate transmission without any form of interference.

Wireless networks, such as worldwide interoperability for microwave access (WiMAX) and W-LANs, suffer from signal degradation after a certain distance. Therefore, the integration of optical OFDM and a microstrip antenna for the last mile is the solution to guarantee the signal reception to the end user in a cost-effective manner.

However, passive microstrip antennas have a limited radiation distance of around 10 m. Increasing the antenna radiation distance, and thus the coverage area, by using an active microstrip antenna is the candidate solution for this constraint.

1.3 Research Objectives

In general, this research focuses on optical OFDM in modern communication systems. In particular, we use Optisystem communication tools to design and simulate a cost-effective optical OFDM based W-LAN system. This proposed optical OFDM system is intended to carry OFDM signals with a 2.4 GHz radio frequency over a cost-effective optical link without using active optical components, such as Erbium-doped fiber amplifier (EDFA) or dispersion compensating fibers (DCFs). Also, an active microstrip patch antenna is analyzed, designed and implemented in the proposed system to extend the wireless coverage area and overcome radiation constraints. These objectives are summarized as follows:

- Modeling and simulation of optical OFDM based wireless LAN.
- Designing a cost-effective system where the signal is processed locally at the CO and no active optical components, such as optical amplifiers, are used in the system.
- Analyzing the microstrip patch antenna, designing and implementing it in the proposed system to extend the wireless coverage area and overcome the radiation constraints.
- Optisystem system is used to design the optical OFDM system, and computer simulation technology (CST) Microwave Studio is used for designing the patch antenna and obtaining the antenna S-parameters and gain, where they are used for representing the antenna in the system.

- To guarantee high system performance and a cost-effective system, a DML, or CW laser, is used as an optical laser source. An external modulator, MZM, is used for higher modulation levels, such as 16 QAM. MMF fiber is used for short optical distance applications, while SMF fiber is investigated for longer optical distance applications up to 80 km without utilizing any optical amplifiers.

- Finally, evaluation and discussion of the system's performance in terms of signal to noise ratio (SNR), optical signal to noise ratio (OSNR), bit error rate (BER), and the equivalent isotropically radiated power (EIRP) are presented.

1.4 Scope of Work

The focus of this research is on optical OFDM based wireless LAN signals for both a single-mode fiber (SMF), for longer distances, and a multimode fiber (MMF), for shorter optical distances. Additionally, this research is involved in using 2.4GHz radio frequency to carry W-LAN signals over an analog optical link and then distributing it wirelessly to the end user using a simple active microstrip patch antenna. The patch antenna is designed for this hybrid optical-wireless link, and the obtained scattering parameters and the antenna gain are implemented in the Optisystem simulations using Touchstone format files. The designed system is cost-effective because the signal is processed locally at the CO, and no active optical components, such as optical amplifiers, are used in the system.

1.5 Methodology

To achieve the proposed objectives, different analysis and design approaches were used. The proposed system consists of four main parts: an OFDM transmitter and receiver, an optical link, a microstrip antenna and a free space path. First, Matlab

software tools and codes were used to analyze the proposed microstrip patch antenna primary dimensions where the patch width and length were obtained. Next, the antenna's dimensions and results were obtained using computer simulation technology (CST) Microwave Studio. Then both transmitting and receiving antenna S-parameters were modified and prepared using Excel spreadsheets that were then tabulated in Touchstone format.

Secondly, all the proposed conventional optical and optical OFDM system blocks were modeled and simulated using Optisystem tools as presented in chapter 4. However, the antenna parameters were not provided by the communication simulation packages such as Optisystem. The only capability provided of these simulation packages was the two-port S-parameter (S2P) component, which was used to implement the microstrip patch antenna parameters. However, the Touchstone format specification was used to load the S-parameters in the Optisystem system. Finally, the simulation results are illustrated, discussed and evaluated regarding EIRP,OSNR, SNR, and BER.

1.6 Dissertation Organization

The rest of the dissertation is organized as follows:

Chapter 2 demonstrates the history, principal, and applications of OFDM as a multicarrier technique for broadband wireless communications. Then, the optical components are reviewed. The principal of optical OFDM is presented in this chapter as well.

Chapter 3 is devoted to the description of basic concepts of a microstrip patch antenna and free space path loss and link budget. In this chapter, the microstrip patch antenna method of analysis and design are provided. Also, the antenna's actual dimensions and

results are obtained using Matlab and CST simulations. The microstrip patch antenna S-parameters, return loss R_L and the gain is calculated. Also, in this chapter, the passive microstrip patch antenna is upgraded by adding a low-power RF amplifier and a bandpass filter to become an active antenna for coverage extension. The free space path loss equations and link budget calculations are discussed and presented. In the next chapter, the designed antenna parameters are used in different models and simulations.

Chapter 4 is divided into three parts. In the first part, a conventional optical wireless system is designed and modeled with the use of QAM as a conventional serial modulation scheme. Then a full optical OFDM based W-LAN system is modeled and simulated using Optisystem tools for downlink and uplink transmissions as presented in the second part. The third part presents a full optical OFDM based W-LAN with an external optical modulator MZM. Of course, the microstrip patch antenna is integrated with an optical system in the three proposed blocks. The results are analyzed and discussed in each part. Also, in this chapter, the effects of the laser source, fiber link, and wireless path on the system performance are discussed. The system performance results are obtained regarding receiving signal constellations, EIRP, SNR, and BER.

Chapter 5 includes conclusions and future work. This chapter is followed by an appendix, which consists of some related tables, figures, and published papers.

Chapter Two: Literature Review

2.1 Multicarrier Techniques vs. Single-Carrier Techniques

OFDM, as a multicarrier modulation scheme, has many advantages over SCM. For example, if SCM schemes, such as GSM or TDMA are used, then the symbol duration decreases with an increase in the data rate, and the multipath fading of the wireless channel will cause more severe ISI [5].

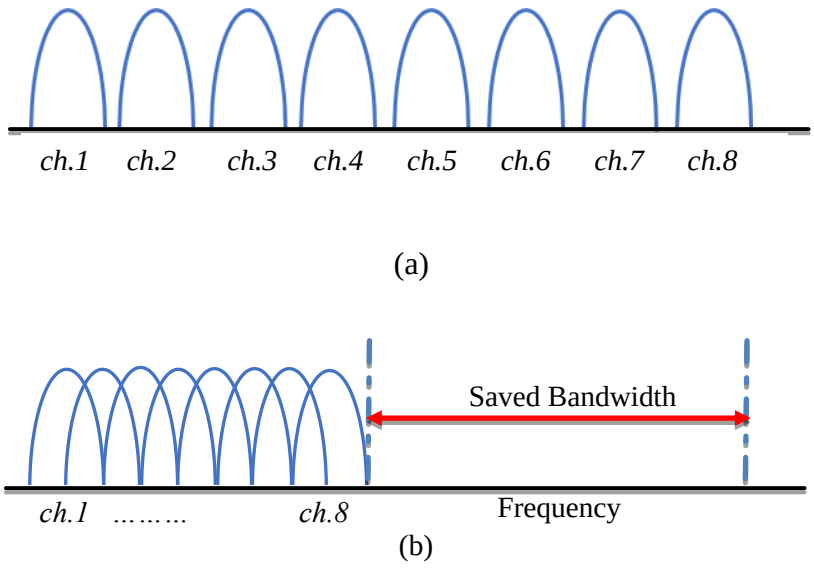

Figure 2.1. The frequency spectrum of eight channels a) utilizing frequency division multiplexing b) The frequency spectrum of OFDM [5].

Hence, OFDM is used in modern wireless applications, such as W-LANs, to combat ISI by dividing the entire channel into many narrowband sub-channels that are transmitted in parallel to achieve high data rate transmissions [7].

Figure 2.1 (a) shows the frequency spectrum of eight channels utilizing frequency division multiplexing (FDM). Parallel transmitters are employed in which guard bands are placed between sub-carriers. In this single carrier technique, a low rate signal is carried over a relatively wide bandwidth channel using a separate carrier frequency for each signal. Those carrier frequencies are spaced adequately to ensure that the signals do not overlap. As shown in figure 2.1 (a), guard intervals or bands are placed between the carriers to ensure that they can be recovered by using bandpass filters at the receiver. The general idea of avoiding spectral overlapping of sub-channels is applied to eliminate intercarrier interference (ICI). However, this technique results in an insufficient utilization of the existing spectrum. Figure 2.1(b) illustrates the frequency spectrum of OFDM subchannels. The OFDM sub-channels are orthogonal to the adjacent channels. The advantage of this technique is that the percentage of the used bandwidth to transmit the same data with FDM is reduced by 50%. However, the advantage of OFDM is reduced if the orthogonality among the subcarriers cannot be maintained between the subcarriers [5].

When single carriers such as FDM or wavelength division multiplexing (WDM) are used in communication applications, information is transmitted on many different frequencies simultaneously [7]. However, there are some main theoretical and practical differences between OFDM and these conventional systems. For example, the subcarrier

frequencies in the OFDM technique are chosen so that the signals are mathematically orthogonal over one OFDM symbol period. Also, the advantage of using inverse fast Fourier transform (IFFT) is that both modulation and multiplexing are achieved digitally, and as a result, the required orthogonal signals can be generated precisely in a reliable efficient way. In FDM or WDM, there are frequency guard bands between the subcarriers. At the receiver, the individual subcarriers are recovered using analog filtering techniques. In OFDM the spectra of individual subcarriers overlap as shown in figure 2.2 where each OFDM subcarrier has a *sin(x)/x2* form. The subcarriers are separated by a fixed frequency spacing Δf. Furthermore, because of the orthogonality property, in a linear channel, the subcarriers can be demodulated without the need for analog filtering to separate the received subcarriers. At an OFDM receiver, the demodulation and demultiplexing process is performed by a fast Fourier transform (FFT). Each OFDM subcarrier has significant sidelobes over a frequency range which includes many other subcarriers. This is the cause of one of the major disadvantages of OFDM: that it is quite sensitive to frequency offset and phase noise. By making the sub-channels narrowband, the individual channels experience almost flat fading; this makes receiver design simpler [5].

2.2 OFDM Technology

OFDM is a new and attractive modulation scheme with efficient bandwidth usage, immune to a multipath fading environment. OFDM is a practical solution to eliminate ICI caused by a dispersive channel. It also has a better spectral efficiency and power efficiency. Nowadays, OFDM is widely used in most new and emerging broadband

wireless and wired communication systems. Very recently, several researchers have shown that OFDM is a promising technology for optical communications [7]. Due to increasing demands for high data-rates in modern communication systems, OFDM has been intensively researched over the last two decades. OFDM as a modulation mechanism provides a high data-rate with robustness against a multipath fading channel [7]. The baseband data in OFDM are distributed among some carriers, making the data symbol long enough to overcome any delay spread that the signal may encounter [3], [4]. OFDM is effectively used in modern communications applications, such as in W-LANs and Wi-Fi [4]. The unique feature of OFDM is the use of orthogonality between the individual subcarriers. Moreover, the importance of OFDM is that it has the best spectral efficiency to RF interference and can also lower multipath distortion [5]. Also, OFDM transfers the complexity of the transceivers from analog to the digital domain [7], [5].

Since Cooley and Tukey formalized and discussed the FFT algorithm in 1965, it has become a popular computational tool [9]. That is because of discrete Fourier transform (DFT) algorithm, it can reduce the complexity of computing the DFT from $O(N^2)$ to $O(N \log N)$. The FFT is a form of the complex DFT, where the term complex means a specific type of mathematics is used. Hence, OFDM is computationally efficient by using FFT techniques to implement the modulation and demodulation functions.

2.2.1 OFDM history

The history of OFDM dates back to the year of 1966, when *Chang* published his paper on the synthesis of band-limited signals for multichannel transmission [10], and followed with a patent for his work in 1970 [11]. This was the first proposal for

generating orthogonal signals based on FFT. He summarized that by presenting a principle for transmitting messages simultaneously through a linear band limited channel without any interference, such as ISI or ICI. In 1971, Weinstein & Ebert implemented the DFT technique for data transmission using the OFDM scheme [12]. The last important aspect of supporting the OFDM scheme is the cyclic prefix (CP), which was proposed in 1980 by Peled and Ruiz [13]. In their proposal, CP replaced the null guards of the OFDM symbol. The main idea of OFDM is to divide the frequency selective channel into some parallel frequency flat subchannels as shown in figure 2.2.

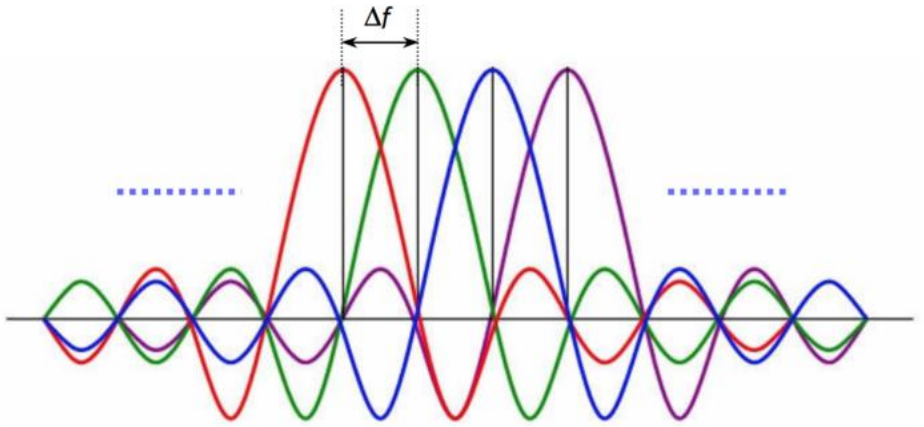

Figure 2.2. OFDM subcarriers spectra

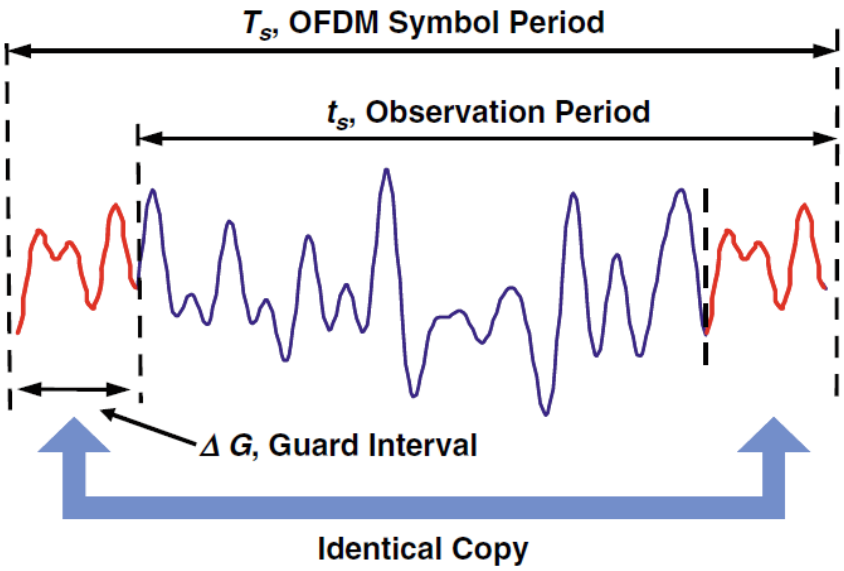

Figure 2.3. Corresponding time-domain OFDM symbol [14]

One of the enabling techniques for OFDM is the insertion of a CP as illustrated in figure 2.3. The figure shows one complete OFDM symbol where a copy of a part of the OFDM symbol is added to the end of the symbol instead of the null guard. Then at the receiver before the FFT block, this CP is removed.

2.2.2 OFDM application

In the last two decades, much work has shown the powerful use of OFDM in both wired and wireless communication networks. OFDM is a strong candidate for the IEEE W-LAN standard and one of the most promising radio transmission techniques for long-term evolution (LTE) [3]. OFDM has already been adopted by many IEEE standard working groups, such as IEEE 802.15.3a [15], which was formed to support high speed, high data rates, low cost, and low power consumption wireless connectivity. Also, OFDM was adopted by the IEEE 802.11a/g/n, the standard for wireless access-point

systems [4]. Ultra-wideband (UWB) technology and orthogonal frequency division multiplexing-ultra-wideband (OFDM-UWB) technology have been widely used in recent wireless communications applications; such as wireless personal area networks (WPANs), W-LANs, and metropolitan area networks (WMANs). Recently, OFDM has been used for optical communication such as optical OFDM.

2.2.2.1 W-LAN

OFDM has evolved over time to where it is today utilized by various standards, such as 802.11 a/g and 802.16 [16-20]. Most W-LANs today operate on a 2.4 GHz spectrum. Deployment started over a decade ago with the initial 802.11 standards and continued with 802.11 b and 802.11 g, as the most popular versions. The 802.11 standards, which utilize 5 GHz frequencies, have been available for many years, but their deployments are uncommon because they do not interoperate with the commonly installed base of 2.4 GHz client devices. Today, with 802.11n beginning to proliferate, the decision to deploy is much tougher. 802.11 n supports both 2.4 and 5 GHz clients. Figure 2.4 shows the spectral mask for a 20 MHz IEEE 802.11 OFDM signal, and the key offsets for this bandwidth are illustrated as well. Table 2.1 summarizes all adopted IEEE 802.11 standards, while Table 2.2 lists all the widely used frequencies for broadband wireless communication systems.

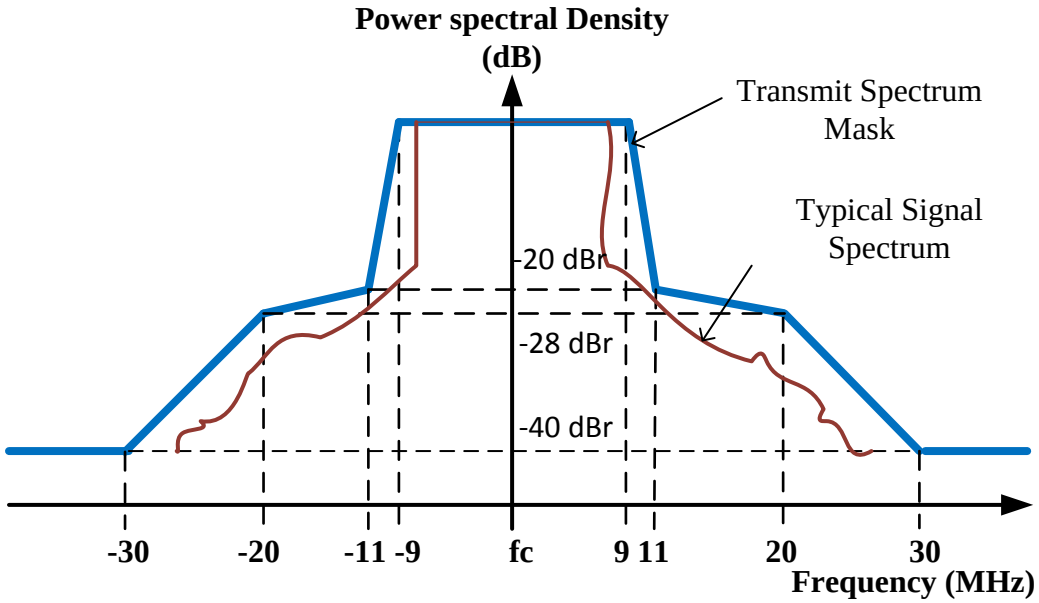

Figure 2.4. Spectral mask measurements on an 80 MHz IEEE 802.11signal

Table 2.1: IEEE 802.11 standards

Wireless Standards	Year of Creation	Freq. band/ bit rate	Pros	Cons
IEEE802.11	1997.	Max **2** Mbps		Too slow.
IEEE802.11b	July 1999.	2.4 GHz up to 11 Mbps	Lowest cost, the signal is good, not easily obstructed, Used for home.	Slowest, maximum speed, home appliances may interfere with the unregulated frequency band.
IEEE802.11a	1999.	5 GHz up to 54 Mbps	Mainly for, fast maximum speed business, no interference.	Highest cost; shorter range signal easily obstructed.
IEEE802.11g	2002/2003.	2.4 GHz up to 54Mbps	Fast maximum speed, signal range is good.	Costs more than 802.11b.
IEEE802.11n	The newest IEEE standard.	2.4GHz/5GHz Over 100 Mbps	Fastest maximum speed and best signal range.	Costs more than 802.11g.

Table 2.2: Frequencies for broadband wireless communication systems

Frequency	Wireless System
2.4 GHz	IEEE 802.11 b/g WALN
5 GHz	IEEE 802.11 a WLAN
2.4 GHz/5GHz	IEEE802.11n WLAN
2-11 GHz (5.8 GHz Normally)	IEEE 802.16 WiMAX

2.2.2.2 MB-OFDM and UWB

UWB and OFDM-UWB technology have been widely used in recent wireless communications applications; such as WPANs, W-LANs, and WMANs [21-28]. By utilizing the conjunction with an optical link, it is possible to transmit ultra-wideband singles at a high data rate over fiber to their intended destination [21], [28].

The multiband orthogonal frequency division multiplexing technique (MB-OFDM) is used in communication applications to increase both the entire system's bandwidth and the data rate transmission. The main benefit of the MB-OFDM is that its demodulation scheme has an inherent capability to mitigate the effects of indoor multi-path interference, thereby allowing very high data rates even under an indoor multi-path environment [24]. The multipath effects of an indoor channel impact the multiband approach to UWB less severely than an impulse radio approach to UWB. The multiband approach to UWB has multiple degrees of freedom over the impulse based approach which can be exploited to reduce receiver complexity [25]. MB-OFDM has been used in UWB-WPAN as a standard for IEEE 802.15.3a [29]. The basic idea of using the MB-OFDM approach is to divide the entire spectrum into 528MHz sub-bands (a total of fourteen across the 3.1 to 10.6 GHz bandwidth) and the data stream is transmitted over

each band by using OFDM subcarriers. The low and high bands for UWB are 3.1 GHz and 10.6 GHz respectively [29-33]. The Federal Communications Commission (FCC) requires that parasitic emission levels must be below -41.3 dBm/MHz in an unlicensed spectrum [26],[27]. The typical advantages of UWB are the low complexity, high data rates, localization and tracking features and coexistence with current narrowband and wideband radio services. The hybrid link presented in [23] consists of two main parts: optical and wireless connection. The optical part interconnects a central office with a UWB distributed antenna. The wireless link provides coverage to wireless ultra-wideband terminals of the indoor environment areas. This technique offers some advantages such as high data rates, low signal attenuation and improved coverage and system performance.

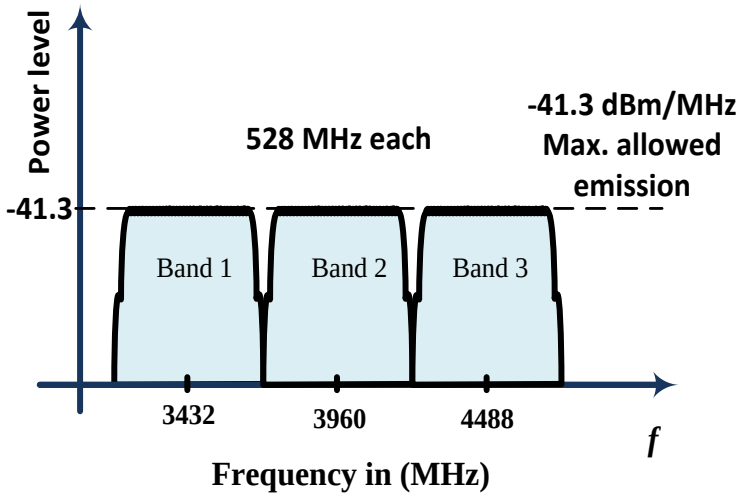

Figure 2.5. UWB frequency of operation [23]

Figure 2.5 illustrates the three lower bands which occupy a bandwidth between 3.168 GHz to 4.752 GHz. Time-frequency coding (TFC) is used to specify the center frequency for transmitting OFDM symbols in a multi-band system. Information is interleaved over three bands by time-frequency interleaving (TFI) code. The center frequencies of the bands #1, #2 and #3 are 3432 MHz, 3960 MHz, and 4488 MHZ respectively [21], [23]. In the MB-OFDM system, the first OFDM symbol is transmitted on band #1, the second OFDM symbol is transmitted on band #3, and the third OFDM symbol is transmitted on band #2 and so on.

In regard to UWB emissions, the FCC states different regulations. UWB signals have a fractional bandwidth of greater than 20% or a UWB bandwidth greater than 500 MHz bounded by points of 10 dB below the highest radiated emission [25].

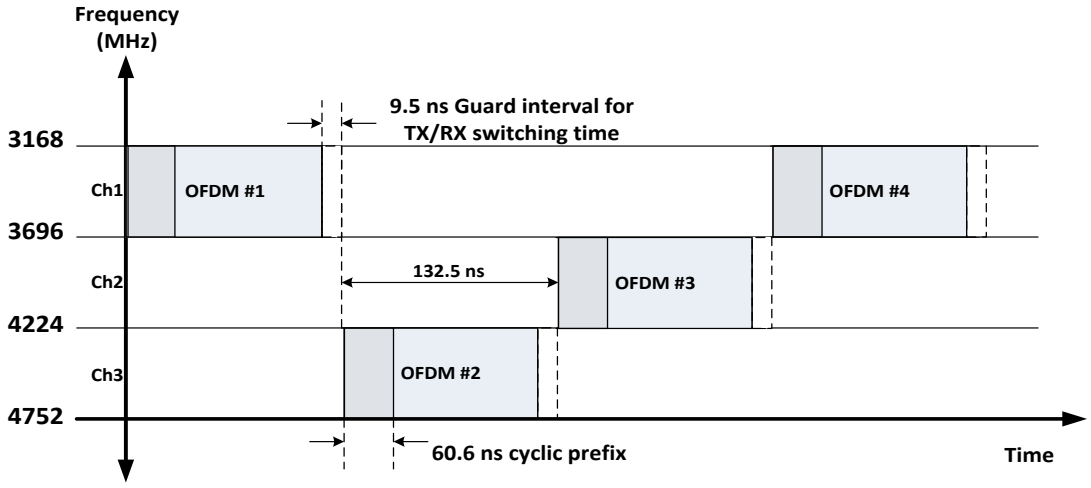

Figure 2.6. MB-OFDM symbols transmission mechanism.

2.2.3 OFDM Advantages

The main advantages of OFDM over other communication techniques are as follows [1]-[3],[8]:

- OFDM makes efficient use of the spectrum by allowing overlap.
- Working on narrowband subchannels makes it easy for OFDM to be more resistant to frequency selective fading compared to SCM ones.
- OFDM overcomes ISI issues.
- Using techniques such as interleaving and adequate channel coding makes it easy to recover symbols lost due to the frequency selectivity of the channel.
- Channel equalization is simpler in OFDM than adaptive equalization techniques in SC systems.
- IFFT/FFT techniques make OFDM computationally stronger and more efficient for modulation and demodulation function implementation.
- OFDM provides a perfect protection scenario against co-channel interference.
- OFDM is different from single carrier systems, where the OFDM output signal at the receiving end is the summation of that which transferred in a considerably large number of orthogonal subchannels.

2.2.4 OFDM drawbacks

OFDM also has some drawbacks that can affect the transmitted signal severely. For example, the transmitted information on one OFDM subchannel can be irremediably lost if a deep fade occurs [34]. Also, if the orthogonality is not adequately warranted by any means, its performance may be degraded due to ISI and ICI. In general, there are

three major issues that can affect any OFDM system if not considered during the system design:

- Frequency offset
- Phase noise
- Peak-to-average-power ratio (PAPR)

2.2.4.1 High peak-to-average power ratio

One of the major disadvantages of OFDM is that the OFDM symbol suffers from the high peak-to-average power ratio (PAPR) [7], [35]. This puts a high demand on linearity in amplifiers. Second, maintaining the orthogonality among the subcarriers keeps the OFDM system secure and avoids interference from occurring. Also, phase noise error can cause some degradation to OFDM symbols. Designing accurate frequency synchronizers for OFDM to reduce the PAPR needs considerable effort. However, several techniques have been proposed such as partial transmit sequences (PTS), selective mapping (SLM), clipping and filtering, coding, tone reservation (TR) and tone injection (TI). Each of these methods has a different cost for the reduced PAPR. For example, in the SLM technique, the transmitter generates groups of adequately different blocks. Each block represents the same piece of information as the original data block, and the transmitter chooses the most favorable blocks for transmission, which bring for the most less PARP effect as shown in figure 2.7, [36], [37]. PAPR can be calculated from the peak - amplitude of the signal waveform divided by the average of the signal:

$$PAPR = \frac{max_n\{|x[n]|^2\}}{E\{|x[n]|^2\}} \tag{2.1}$$

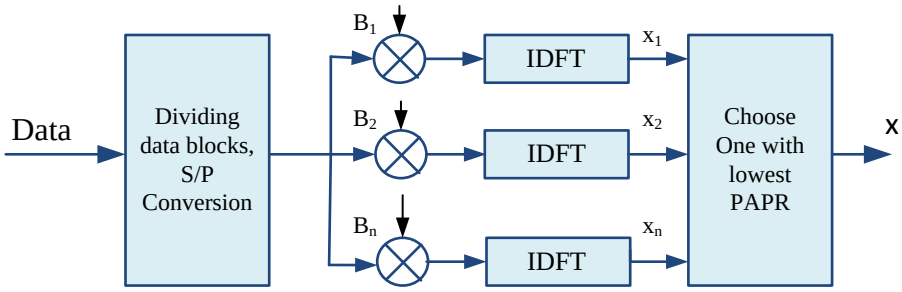

Figure 2.7. SLM technique block diagram [36]

2.2.4.2 Synchronization and loss of orthogonality effects on OFDM symbols

The advantage of OFDM is very useful only when orthogonality is strongly maintained. In cases where orthogonality is not adequately guaranteed by any substance, its performance may be reduced due to ISI and ICI. However, OFDM signals can be affected by either or both of these problems: symbol time offset (STO) or carrier frequency offset (CFO). An OFDM symbol can occur as shown in the figure 2.8 below. Depending on the location of the estimation of the beginning point of the OFDM symbol, the effect of STO might be different [3], [7]. This estimation can be summarized in four different cases of timing offset as shown in figure 2.8. Let's consider that τ_{max} is the lagged channel response of the multi-path delay spread.

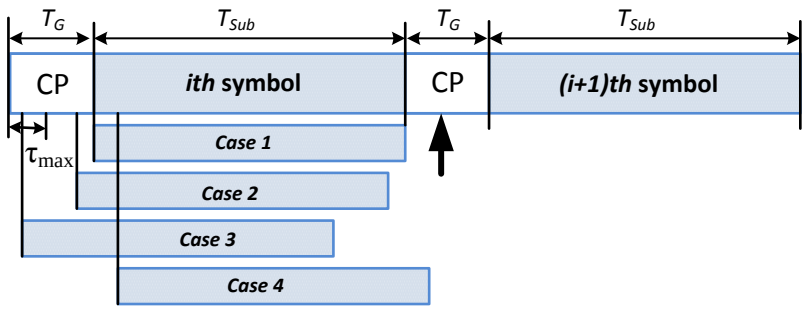

Figure 2.8. Effect of SOT: four different cases of OFDM symbol starting point [3].

Case 1: In this case, the beginning point of the OFDM symbol coincides with the exact timing which goes to preserving the orthogonality among subcarrier frequency components. Hence, the OFDM symbol can be perfectly recovered at the receiver without any influence of ISI, ICI or STO.

Case 2: In this case, the beginning point of the OFDM symbol starts before the exact period and after the lagged channel response to the previous OFDM symbol with the accurate timing which can preserve the orthogonality among subcarriers frequency components. There is no overlap between the two OFDM symbols as indicated in figure 2.9, which means ISI cannot exist. However, there exists a phase offset that is relative to the STO forcing the signal constellation to be revolved around the origin as indicated in figure 2.9b.

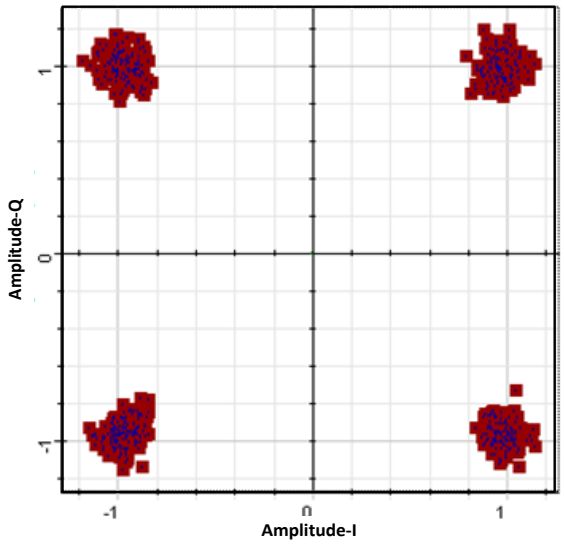

a)

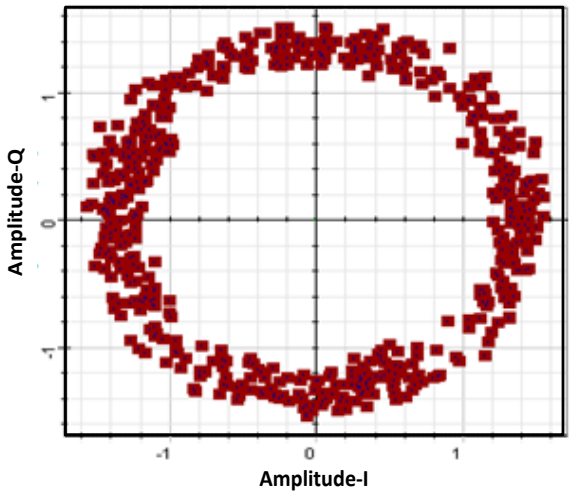

b)

Figure 2.9. Effect of SOT on receiving OFDM constellation signal. a) Signal constellation is not affected by STO. b) Signal constellation affected by SOT [38].

Case 3: In this case where the starting point of the OFDM symbol is estimated to exist before the end of the lagged channel response to the previous OFDM symbol, there is no

chance to avoid ISI occurring. Therefore, the orthogonality among the subcarriers is destroyed by the ISI, and ICI occurs.

Case 4: This is the case when the starting point of the OFDM symbol is estimated to exist after the exact point, which leads to a huge destruction in orthogonality and ICI occurs.

2.3 Optical Elements

Transmitting the optical signal from end-to-end involves both electrical and optical signal paths. An optical source is required to perform conversion from the electrical to the optical domain, while to perform the conversion in the opposite direction from the optical to the electric an optical receiver is used. In general, an optical link consists of three main parts: optical transmitter, optical fiber and optical receiver as shown in figure 2.10.

Figure 2.10. General optical link components.

From a simplistic point of view, the function of an optical fiber link is to transport a signal from some piece of electronic equipment (e.g., a computer, telephone, or video device) at one location to similar equipment at another location with a high degree of

reliability and accuracy [14]. Figure 2.10 shows the key sections of an optical fiber communications link, which are as follows [39], [40]:

2.3.1 Optical sources.

An optical transmitter consists typically of a light source and associated electronic circuitry. The source can be a light-emitting diode (LED), in which spontaneous recombination dominates, or a semiconductor laser diode (LD), in which the stimulated emission is a dominating mechanism [41-44]. The electronic circuitry is used for setting the source operating point, controlling the light output stability, and varying the optical output in proportion to an electrically formatted information input signal. The main function of an optical source is to convert received electrical signals to optical forms, then launch the modulated signal into the optical fiber. However, many laser sources can be used for stimulated emission in optical systems. The simplest laser structure is the *Fabry-Perot laser (FPL)* type. This type is only used for low-speed optical communications and can also be applied to CD players, where some variations in the center wavelength can be tolerated. The second type is the *distributed feedback (DFB)* laser. DFB is a special type of edge-emitting laser, and it is optimized for single mode operation. Moreover, the spectral width of the DFB laser is very narrow, which is ideal for WDM applications. The third LD type is the *vertical-cavity surface-emitting laser (VCSEL*) [44]. The VCSELs are highly promising laser sources for ultra-low-cost intensity modulated-direct detection (IMDD) optics, which can be produced at extremely low cost mainly due to the reduced manufacturing processes involved [8].

In general, there are three basic processes in semiconductor materials by which the light interacts with matter [42-44]:

- Absorption
- Spontaneous emission
- Stimulated Emission

In optical systems, the received information modulates the optical signal generated by a laser source before being transmitted over the optical fiber. This can be accomplished directly by modulating the bias current of the semiconductor laser, or instead, the LD is usually biased at s constant current to provide CW output. External modulators are used to impose the carried data signal to be transmitted [44-46]. The most popular modulators are electro-optic optical modulators, such as Mach–Zehnder modulators (MZM), and electroabsorption modulators. The main role of these modulators is to increase the transmitted optical power in the fiber in case high data rates are generated.

2.3.2 Optical links.

Optical fibers serve as a medium to carry the optical signal from the source to its destination. Utilizing the benefit of large bandwidth and low loss allows high-speed signals to be transmitted over long distances before regeneration is needed. The optical fiber is manufactured from several different materials, including pure silica, which is mixed with different dopants to modify the refractive index of the optical fiber [44], [45]. In general, an optical fiber consists of two primary layers, the core and the cladding, protected by buffer coating.

Also, the optical fiber is placed inside a cable that offers mechanical and environmental protection. A variety of fiber types exist, and there are many different cable configurations which depend on whether the cable is to be installed inside a building, in underground pipes, outside on poles, or underwater. In general, there are two types of optical fiber: MMFs, which are used for short distances, or SMFs, which are used for long-haul distances. MMF has a core size of 50-100 μm typically, while SMF allows only one mode and has a core size of about 9μm which eliminates intermodal dispersion, and as a result, can support transmission over longer distances [41-44].

2.3.3 Optical receivers.

The common photodiodes are *p–i-n* photodiode (pin), avalanche photodiode (APD), and metal–semiconductor–metal (MSM) photodetectors [41-43]. The most widely used semiconductor photodetector is the p-i-n photodiode type, shown in figure 2.11. The pin photodiode consists of p and n regions separated by a very lightly n-doped intrinsic (*i*) region. In this type of photodetector, a sufficiently large reverse bias voltage is applied to the device. The reverse bias ensures that the intrinsic region is depleted of any charge carrier.

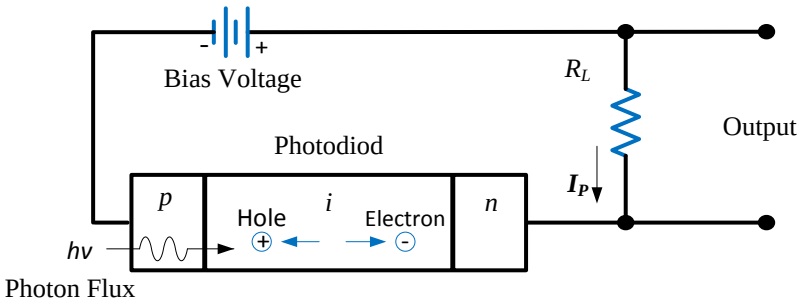

Figure 2.11: PIN photodetector schematic diagram [44], [46].

Inside the receiver is a photodiode that detects the degraded and distorted optical signal emerging from the end of an optical fiber. The major role of the photodetector is to receive the output optical power of the fiber for detection and convert it to electrical power in terms of electrical current. The shot and thermal noise components are also added to the received signal. The photocurrent of the photodiode would be simply expressed by [39]:

$$I_{pd} = \mathcal{R}P_0 + I_{th} + I_q + I_{dk} \tag{2.2}$$

Where I_{th} and I_q are the thermal and shot noise components, respectively, and the photodiode responsivity $\mathcal{R}$ *and* I_{dk} is the average dark current. Normally, its value is in nano-amperes and can be obtained from the photodiode datasheet. Dark current is the minimum detectable signal through the photodiode in the absence of light, when it operates in the photoconductive mode. It depends on operating temperature, bias voltage and the type of detector. Dark current is also the source of noise when a photodiode is used in an optical communication system.

The performance of a photodiode is often characterized by the responsivity $\mathcal{R}$ which is related to the quantum efficiency by η:

$$\mathcal{R} = \frac{I_P}{P_{in}} = \frac{\eta q}{h\nu} \tag{2.3}$$

Figure 2.12 provides a comparison of the responsivity and quantum efficiency as a function of wavelength for pin photodiodes constructed of different materials. From figure 2.12, it is clear that the responsivity parameter is very important for the determination of which material can be used for required application based on the photocurrent generated per unit of optical power.

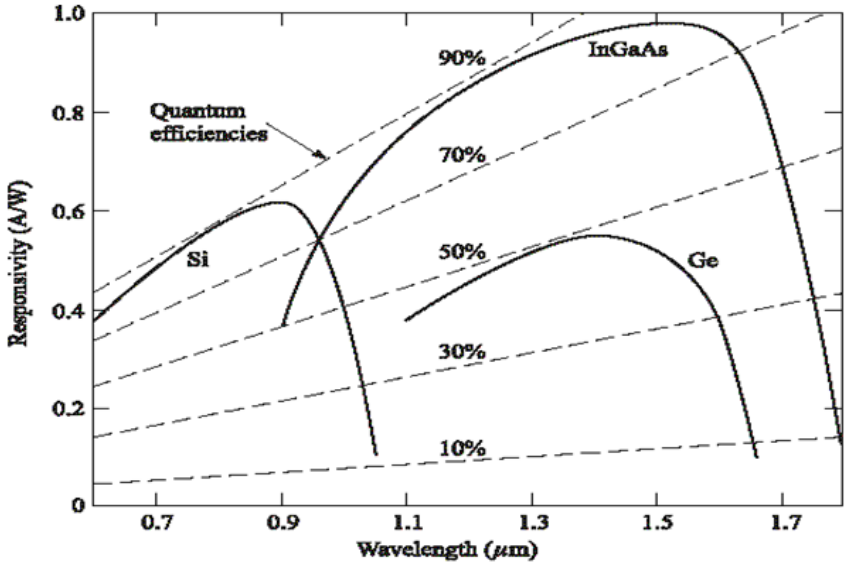

Figure 2.12. Responsivity vs. wavelength [43-44]

Analogous to the pin photodiode, the performance of an APD is characterized by its responsivity R_{APD}, which is given by [44]:

$$\mathcal{R}_{APD} = \frac{nq}{hv} M = \mathcal{R}M \tag{2.4}$$

where $\mathcal{R}$ is the unity gain responsivity, and $M=I_M/I_P$, where I_M is the average value of the total multiplied output current, and I_P is the primary unmultiplied photocurrent.

2.3.4 Dispersion effects in optical fibers

A transmitted pulse along an optical fiber spreads out after a certain distance and loses part of its energy. This pulse spreading is continuous over the length of the fiber span, and it spreads out and continues as well as the pulse travels through optical glass. For example, this pulse spreading in SMFs is mostly caused by chromatic dispersion, which is a result of different frequencies of light traveling at different velocities through an optical link [44]. The laser sources produce optical pulses with different frequencies

and the wider the spectral width, the more optical frequencies the pulse contains and the faster it will spread.

- **Chromatic dispersion**

Chromatic dispersion (CD) is caused by the difference in velocities among different spectral components within the same mode. Chromatic dispersion results from the combination of the effects of material and waveguide dispersion. However, material dispersion results in the spreading of an optical pulse due to the different speeds of the optical frequencies that produce that pulse. Waveguide dispersion refers to differences in the signal speed depending on the distribution of the optical power over the core and cladding of the optic fiber. Material dispersion and waveguide dispersion are likely to have opposite effects as shown in figure 2.13. However, chromatic dispersion is a broadening of the input signal as it travels down the length of the fiber.

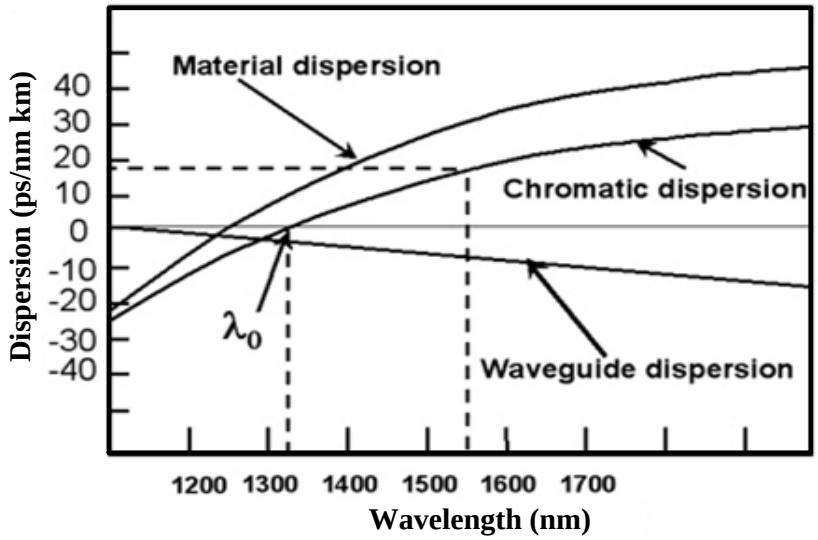

Figure 2.13. Chromatic dispersion is the combined result of material dispersion and waveguide dispersion, which tend to have opposite effects [44],[47].

Mostly, laser sources are used in long-distance fiber optic links, and they have a very narrow spectral width. Also, fibers are optimized for the wavelength of use, which depends on the application of interest. Nonetheless, both mentioned factors minimize the effects of chromatic dispersion, but cannot entirely get rid of it. As the pulse travels along the fiber, the light of longer wavelength travels slightly faster and spreads the pulse out as indicated in figure 2.14.

Figure 2.14. effect of dispersion on an optical pulse in a fiber link

2.3.5 Optical link power budget

The system's power, gains, and losses for both the transmitter and receiver are the main parameters that can affect any communication link's performance. Hence, calculating the system's link budget is an essential task for engineers to establish a solid base in any future optical project. Figure 2.15 shows the optical power budget calculations from the transmitter to the receiver including the link margins and receiver sensitivity. The losses happen for the fiber and connectors that connect the fiber to other components. In any optical link project, the fiber losses should be considered, and the losses count for different fiber types, lengths, and operating wavelengths. For example, for MMFs, the loss is about 3 dB/km for 850 nm laser sources, while 1 dB/km for 1300

nm laser source. In the case of SMFs, the loss decreases and is about 0.5 dB/km for 1310 nm sources, and 0.4 dB/km for 1550 nm.

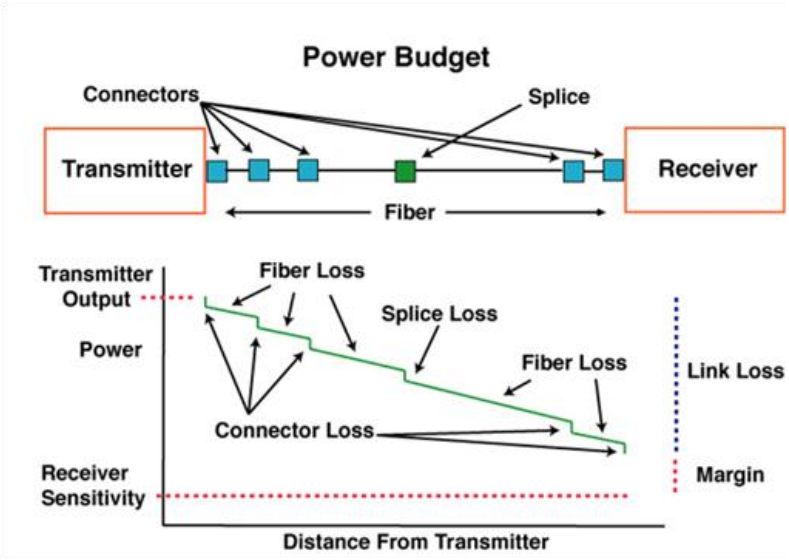

Figure 2.15. Power budget vs. distance from the transmitter [48].

2.4 Radio over fiber principal

Radio over fiber (RoF) uses highly linear optical fiber connections to distribute RF signals from a central station to RAUs. Functions such as coding, multiplexing, and modulation can be performed at the central location. Also, because of the high bandwidth (50-THz) transmission medium and the low loss of the optical fiber (0.2 dB/km) at 1.55 micrometers, system complexity is reduced and shifted away from the antenna. In a RoF system, the input signal is applied to a laser diode where it modulates the intensity of the output light. This light has wavelengths of either 1,300 nm or 1,550 nm of low transmission loss. The fiber may be a multimode or a single mode, where the latter is preferred for link spans of a couple of hundred of meters for its low dispersion properties.

The optical receiver usually consists of a p-i-n photodiode, which provides an RF power output proportional to the square of the input optical power. So, for reasons of simplicity and cost, IM-DD is used for cellular applications [49]. Figure 2.16 shows the typical components of a radio-over-fiber system.

The analog optical links, by nature, suffer from impairments such as noise and distortion. The dominant distortion in the system arises from the laser source in most cases. The RoF has been recently used in cable TV networks [7], and it has also found its way in optical networks along with the mobility of wireless networks [39].

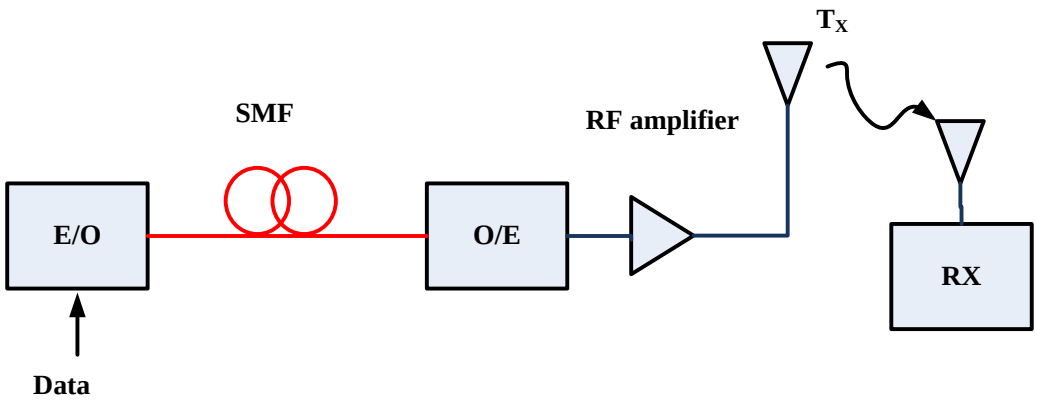

Figure 2.16 Typical implementation of a radio-over-fiber system [49].

2.5 Optical OFDM concepts

In general, two scenarios have been used to carry optical OFDM signals. The first proposed scenario is the direct-detection optical OFDM (DD-OOFDM) [50]. The second one is the coherent detection, where the received signal is mixed locally with a generated

carrier signal as in coherent optical OFDM (CO-OFDM) [7], [14], [51]. Both techniques have advantages. DD-OOFDM has a simple receiver, but some optical frequencies must be unused if unwanted mixing products are not to cause interference. This is usually achieved by inserting a guard band between the optical carrier and the OFDM subcarriers. However, using it that way possibly reduces the spectral efficiency. DD-OOFDM also requires more transmitted optical power, as some power is required for the transmitted carrier. *Brendon et al*. [52] demonstrated three versions of DD-OOFDM, and all have different levels of complexity at the transmitter, but only a single photodiode for direct detection was used. Also, compensating for chromatic was used and it was shown that the DD-OOFDM systems are tolerant of linear imperfections.

CO-OFDM requires a laser at the receiver to generate the carrier locally and is more sensitive to phase noise [53]. CO-OFDM requires coherent reception, and because of the sensitivity of OFDM to frequency offset [6] and phase noise, very narrow line-width lasers are required at the transmitter and receiver, and sophisticated tracking algorithms are required to track laser frequency and phase [54]. There is currently extensive research into the performance of both systems and on techniques to mitigate the disadvantages of each system [7], [55-59].

Chapter Three: Microstrip Patch Antenna Design and Free Space Link

3.1 Introduction

Microstrip patch antennas are simple, lightweight, inexpensive and have a low profile. As a result, they have received considerable attention since the 1970s [60]. Also, these low-profile antennas can be used in many government and commercial applications, such as mobile radio and wireless communications that have similar specifications. The aim of designing a microstrip patch antenna is to get scattering parameters (S-parameters) values. Those S-parameters will be implemented in the Optisystem tool for optical OFDM to represent the designed microstrip patch antenna.

Antenna parameters are not provided by communication simulation packages such as Optisystem. The only capability provided by these simulation packages is the two-port S-parameter (S2P) component that can be used to implement the antenna parameters. From the literature, one of the best software tools for designing small antennas for broadband applications is CST Microwave Studio. Because it uses the time domain method; and the range of simulation methods in CST MWS allows engineers to choose the best technique for each application [61]. For the reasons mentioned above, we adopted this simulation tool to design the photonic antenna and obtain the scattering parameters to be implemented later in the system. This chapter discusses in detail the analysis and design steps of the microstrip rectangular patch antenna. The free space path loss and the wireless link budget are also presented.

3.2 Microstrip Patch Antenna

The idea of a microstrip patch antenna can be traced to 1953 [62] and a patent in 1955 [63]. Microstrip antennas have received considerable attention since the 1970s [60], [64]. In general, microstrip antennas consist of a very thin metallic patch ($t \ll \lambda_0$) placed on a substrate with a dielectric constant ε_r as shown in figure 3.1. The substrate is above a ground plane with a height of $h \ll \lambda_0$ and usually $0.003 \leq h \leq 0.05\lambda_0$. The patch is made from a very thin layer of conducting material. The microstrip patch can have different shapes such as square, rectangular, dipole, and circular.

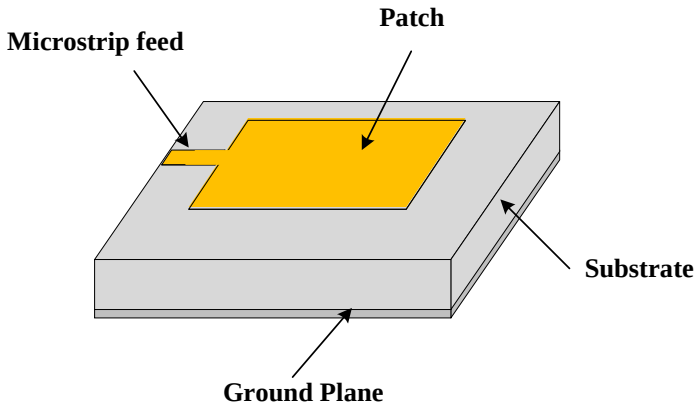

Figure 3.1. Microstrip antenna structure

For example, in the case of a rectangular patch, the length L of the patch is usually between $\lambda_0/3$ and $\lambda_0/2$, in other words, $\lambda_0/3 < L < \lambda_0/2$. The microstrip patch and the ground plane are separated by a dielectric substrate as illustrated in figure 3.1. Unremarkably, the used dielectric substrates are in the range of $2.2 \leq \varepsilon_r \leq 12$. The thickness of a substrate is very important for designing an antenna with better performance. A thick substrate whose dielectric constant is at the lower end of the range

($2.2 \leq \varepsilon_r \leq 12$) can provide better efficiency, larger bandwidth, loosely bound fields of radiation into space. However, it has a penalty of larger antenna size. On the other hand, a thin substrate with a high dielectric constant is desirable for designing a microstrip patch antenna. Tightly bound fields are required to minimize undesired radiation, coupling and leads to smaller patch sizes. They are less efficient and result in narrower bandwidth and a compromise is needed between antenna performance and dimensions. [65].

There are many configuration ways to feed microstrip antennas. The most common ways are the microstrip line, coaxial probe, aperture coupling, and proximity coupling. The microstrip line feed is easy to fabricate, simple to match by controlling the inset position and simple to model.

3.2.1 Methods of analysis

The common methods for analyzing microstrip patch antennas are [65]:

- The transmission line model,
- Cavity model, and
- Full wave model.

The easiest method among these models is the transmission line model. This method gives good physical insight, but it is less accurate compared to the cavity and full wave models.

3.2.2 Microstrip patch antenna analysis

The transmission-line model method is applied in this work for designing a microstrip patch antenna. Microstrip patch antennas can have any shape, but the most widely used configuration is the rectangular patch. It is very easy to design and fabricate using the transmission line model.

The rectangular microstrip patch antenna is as shown in figure 3.2. From the figure, we can see that the rectangular patch consists of a radiating patch and a ground plane. The patch is made from copper or gold conducting materials. To reach a higher antenna performance, a thick dielectric substrate with a low dielectric constant is required since this grants a larger bandwidth, better efficiency, and better radiation.

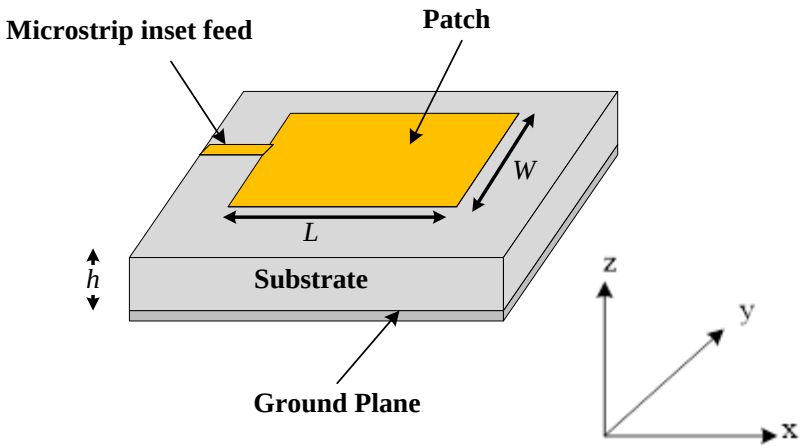

Figure 3.2. Microstrip patch antenna geometry [66].

The microstrip is a nonhomogeneous line which has two different dielectrics: the substrate and air. Finding the effective dielectric constant (ε_{reff}) is very important in order to calculate the wave propagation in the line and the effective patch length (L_{reff}). Therefore, the ε_{reff} can be calculated by the following equation [67-68].

$$\varepsilon_{reff} = \frac{\varepsilon_r + 1}{2} + \frac{\varepsilon_r - 1}{2}\left[1 + 12\frac{h}{W}\right]^{-\frac{1}{2}} \tag{3.1}$$

Where,

ε_r is the dielectric substrate constant;

h is the height of the dielectric substrate, and

W is the width of the patch.

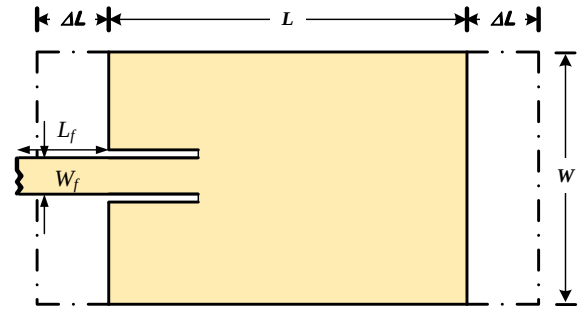

(a) Top view of the patch

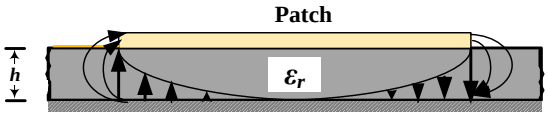

(b) Side view of the patch

Figure 3.3 Physical and effective lengths of a rectangular microstrip patch [65].

A practical width (*W*) that leads to good radiation efficiencies is:

$$W = \frac{c}{2f_r\sqrt{\frac{(\varepsilon_r+1)}{2}}} \tag{3.2}$$

Where *c* is the speed of light in free-space, and f_r is the operating frequency (resonant frequency)

From figure 3.3, it can be seen that the length of the patch is extended by *ΔL* at both ends. This results in fringing effects. The patch of the microstrip antenna looks greater than its physical dimensions. In fact, the extended length is a function of the effective dielectric constant ε_{reff} and width to height ratio (*W/h*) and can be calculated as follows [69]:

$$\Delta L = 0.412 * h * \frac{(\varepsilon_{reff}+0.3)(\frac{W}{h}+0.264)}{(\varepsilon_{reff}-0.258)(\frac{W}{h}+0.8)} \tag{3.3}$$

Now the effective length of the patch is:

$$L_{eff} = L + 2\Delta L \tag{3.4}$$

Where $L = \lambda/2$ for a dominant TM_{010} mode with no fringing.

For a given resonance or radio frequency f_r, the effective length is:

$$L_{eff} = \frac{c}{2f_r\sqrt{\varepsilon_{reff}}} \tag{3.5}$$

Where c is the speed of light in free space, and thus, the patch length can be calculated by equation (3.6) as follows:

$$L = \frac{c}{2f_r\sqrt{\varepsilon_{reff}}} - 2\Delta L \tag{3.6}$$

The transmission line model is applied only to infinite ground planes. The finite ground planes can be obtained if the size of the ground plane is greater than the microstrip patch dimensions by approximately six times the substrate height. The ground plane dimensions L_g and W_g can be calculated as in the following equations:

$$L_g = 6h + L \tag{3.7}$$

$$W_g = 6h + W \tag{3.8}$$

The feed point used in this design is given by the coordinates (X_f, Y_f) from the origin. The feed point must be located at the point on the patch where the input impedance is 50 Ω for the resonant frequency. As mentioned earlier, the aim of designing this antenna is to be applied to an optical link. Hence, the photodiode will be integrated with this microwave patch antenna, and the photocurrent generated by a photodiode directly excites the antenna.

3.2.3 Microstrip antenna design and results

The essential parameters for designing a microstrip patch antenna are the operating radio frequency (f_r), the dielectric substrate height (h), and dielectric constant (ε_r). The selected operating radio frequency (antenna resonant frequency) is 2.4 GHz. The used dielectric substrate material is *FR4* (FR4 is a grade designation for glass epoxy laminates and is the grade most widely used today) with a height of 1.6 mm, where the dielectric constant of this material is ε_r =4.5. The microstrip patch antenna design is similar to those procedures in [70], [71], [65].

After the essential parameters f_r, (in Hz), ε_r and h are specified, the patch width W and length L must be determined. Mathlab tools were used to calculate the microstrip patch antenna parameters. The essential parameters are used to analyze the initial dimensions of the patch antenna.

Table 3.1 Microstrip patch antenna geometry parameters.

Microstrip antenna parameters	Analyzed dimensions (mm)
Material used	FR4
Dielectric constant (ε_r)	4.5
Antenna height (h)	1.6 mm
Rectangular patch dimensions (W)	37.6 mm
Rectangular patch dimensions (L)	28.6 mm
Substrate width, (W_g)	47.29 mm
Substrate length, (L_g)	38.73 mm
Inset feed dimension, (W_f x L_f)	0.99x7.8 mm^2

The patch antenna was designed based on the equations listed above and optimized by using CST Microwave Studio. Many optimization iterations were applied

until the final result for the operating frequency was obtained, and the summary of analyzing dimensions is listed in Table 3.1.

The dimension of the microstrip patch antenna was obtained, and the scattering parameters were collected. Meanwhile, the transmitting and receiving antenna's gain was obtained, and it is about 3 dBi. Also, the relationship between the return loss |*S11*| in dB and the RF frequencies is illustrated in figure 3.6. The minimum return loss (R_L) value at the 2.4 GHz RF center frequency is-26.6 dB from figure 3.4.

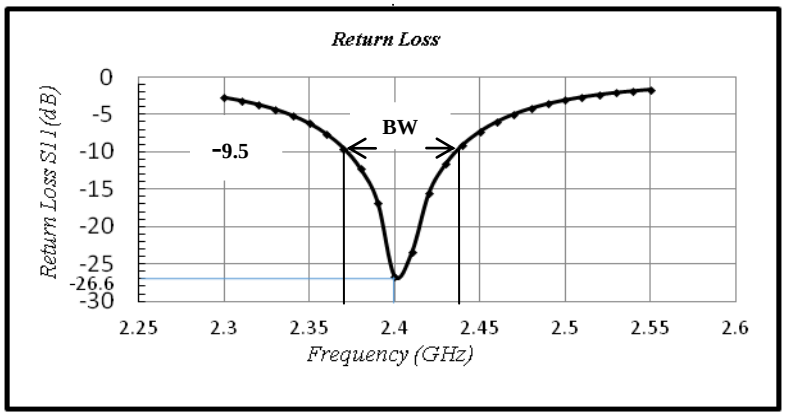

Figure 3.4. Antenna return loss $|S_{11}|$ vs. RF frequency [66]

The bandwidth can be the range of frequencies on either side of the center frequency as shown in figure 3.4. For perfect matching between the transmitter and the antenna, the reflection coefficient $\Gamma = 0$ and $R_L = \infty$, which means no power would be reflected back, whereas a $\Gamma = 1$ has an $R_L = 0$ dB, which implies that all incident power is reflected. To ensure good antenna performance, the R_L should be greater than -9.5 dB [72].

3.2.4 S-Parameters and antenna gain relationship

H, Y and Z parameters, as mentioned in chapter 2, are not suitable for radio and microwave parameters. These parameters require continuous adjustment because of the changing of the SWR over a range of frequencies. The scattering matrix gives a representation more in accord with direct measurements and the ways of incident transmitted and reflected waves. Like impedance or admittance matrix for an N-port network, the scattering matrix provides a perfect overview of the network as seen in its N-ports as depicted in figure 3.5. The impedance and admittance matrices are obtained from the currents and voltages at the ports, while the scattering matrix relates the voltage waves incident on the ports to those reflected from the ports.

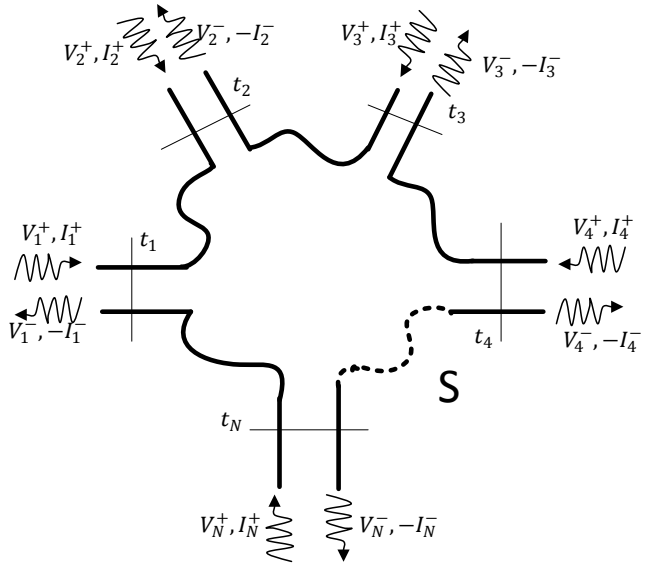

Figure 3.5. An arbitrary *N*-port microwave network [73]

The scattering matrix or S-matrix describes the relationship between the amplitudes of the voltage wave incident on port n (V_n^+) and the amplitudes of voltage wave reflected from port n (V_n^-) as:

$$\begin{bmatrix} V_1^- \\ V_2^- \\ \vdots \\ V_N^- \end{bmatrix} = \begin{bmatrix} S_{11} & S_{12} & \cdots & S_{1N} \\ S_{21} & & & \vdots \\ \vdots & & & \\ S_{N1} & \cdots & & S_{NN} \end{bmatrix} \begin{bmatrix} V_1^+ \\ V_2^+ \\ \vdots \\ V_N^+ \end{bmatrix}, \tag{3.9}$$

Or, it can be written in matrix form as:

$$[V^-] = [S][V^+] \tag{3.10}$$

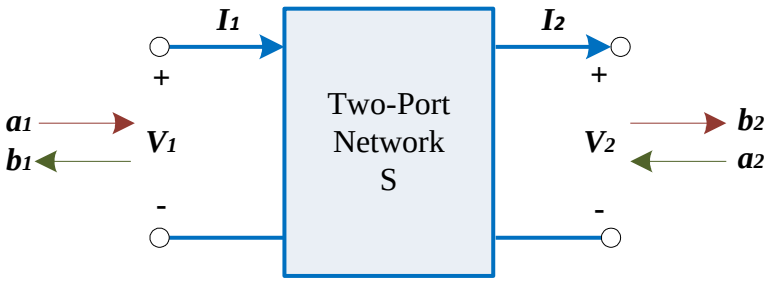

Figure 3.6. Two port network

Figure 3.6 shows the typical two-port network. This linear two-port network can be characterized by equivalent circuit parameters which are two-dimensional scattering matrix. Hence scattering parameters (s-parameters) can be determined as shown in figure 3.7.

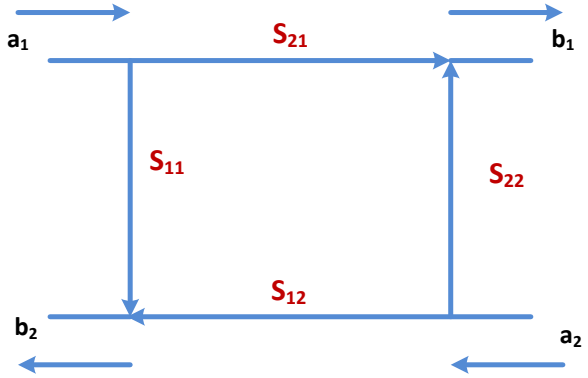

Figure 3.7. Two port network represented by S-parameters

the scattering matrix is [73].

$$\begin{bmatrix} b_1 \\ b_2 \end{bmatrix} = \begin{bmatrix} S_{11} & S_{21} \\ S_{12} & S_{22} \end{bmatrix} \begin{bmatrix} a_1 \\ a_2 \end{bmatrix} \tag{3.11}$$

or

$$\begin{aligned} b_1 &= S_{11}a_1 + S_{12}a_2 \\ b_2 &= S_{21}a_1 + S_{22}a_2 \end{aligned} \tag{3.12}$$

Where a indicates incident powers and *b* indicates reflected powers.

The relationship between the equivalent isotropically radiated power (*EIRP*) and antenna accepted power P_t is given by equation (3.13.) [71], [72], [74].

$$EIRP = G_p.P_t \tag{3.13}$$

Where G_p and P_t are the antenna gain and the antenna accepted power, respectively.

The scattering parameters $|S_{21}|$ also can be defined mathematically by using the antenna gain G_p and the S_{11} as follows:

$$|S_{21}| = \sqrt{Gp(1 - |S_{11}|^2)} \tag{3.14}$$

Also, the antenna gain can be derived from S_{21} and S_{11} for the transmitting antenna as given in equation (3.15)

$$G_p = \frac{|S_{21}|^2}{1-|S_{11}|^2} \tag{3.15}$$

Therefore, using the antenna return loss parameter S_{11}, it is possible to find other scattering parameters and antenna gain mathematically. After the s-parameters are obtained, they must be converted to Touchstone format files. These Touchstone format files contain all the required information for the microstrip patch antenna such as antenna return loss R_L, gain G_P, operating frequency f_r and the S-parameters. These files are uploaded into the Optisystem tools as is seen in chapter 4.

In addition, the obtained scattering parameter files for transmitting and receiving antennas are listed in Appendix A as transmitting.s2p and receiving.s2p, respectively.

3.3 Active Microstrip Patch Antenna

In conventional microwave antennas, microwave power is transmitted to and from the using RF cable. In photonic antennas, the RF cable is replaced with optical fiber, and it is necessary to use optoelectronic components, such as laser diodes and photodiodes, for the conversion of the radio signal to an optical signal and vice-versa. The passive microwave patch antenna has a limited radiation distance that is considered a major drawback in wireless communication networks. Hence, in this work, the passive microwave antenna is modified to an active microstrip patch antenna by combining a low radio power amplifier with a band-pass Gaussian filter to the antenna to increase the antenna coverage area. The used low power amplifier has a gain of 20 dB, and the band-pass Gaussian filter has a bandwidth of 70 MHz. The noise figure (NF) of the RF

amplifier is 4.8 dB and noise power of -170 dBm is included [66]. The active microstrip patch antenna is illustrated in figure 3.8. The active photonic antenna concept has been in use in microwave engineering for a number of years [70]. An active photonic antenna operating at 2.4 GHz wireless over fiber system was proposed in [74],[75] and different design techniques were presented in [67]. [75-76].

Photonic antennas can be divided into two types: hybrid or monolithic. A hybrid photonic antenna consists of two independent parts: a fiber-optic photodiode module and a conventional microwave antenna. These are connected by microwave connectors. In the monolithic-photonic antenna, the photodiode is integrated with a microwave antenna, and the photocurrent generated by the photodiode directly excites the antenna. Photonic monolithic antennas have the following advantages [77]:

- Lightweight and small size as a photonic antenna does not require metal RF cables and connectors;
- The possibility of remote antenna control due to low loss in optical fiber below 0.2 dB/km;
- Wide bandwidth, which is limited only by the antenna itself;
- Immunity to electromagnetic interference, which is important to large antenna systems;
- The possibility of using optical signal processing and optical generation of microwaves in antenna systems.

It should be noted that only the transmitting photonic antenna can be constructed based on the photodiode due to the unilateral nature of the optoelectronic components.

The main disadvantages of the transmitting photonic antenna are:

- Relatively low output microwave power, limited by maximal photocurrent generated by the photodiode, which is usually not more than tens of milliamperes, and
- Optoelectronic conversion loss, which can exceed 10 dB.

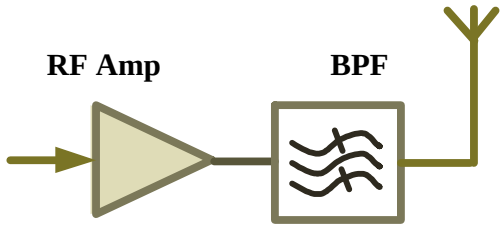

Figure 3.8. Active microstrip patch antenna structure [71]

Figure 3.9 shows the design procedure for the proposed microstrip patch antenna used in the system. The antenna scattering parameters are formed in Touchstone format files which are loaded into the Optisystem communication tools [78]. The obtained scattering parameter files for transmitting and receiving antennas are listed in Appendix as transmitting.s2p and receiving.s2p respectively.

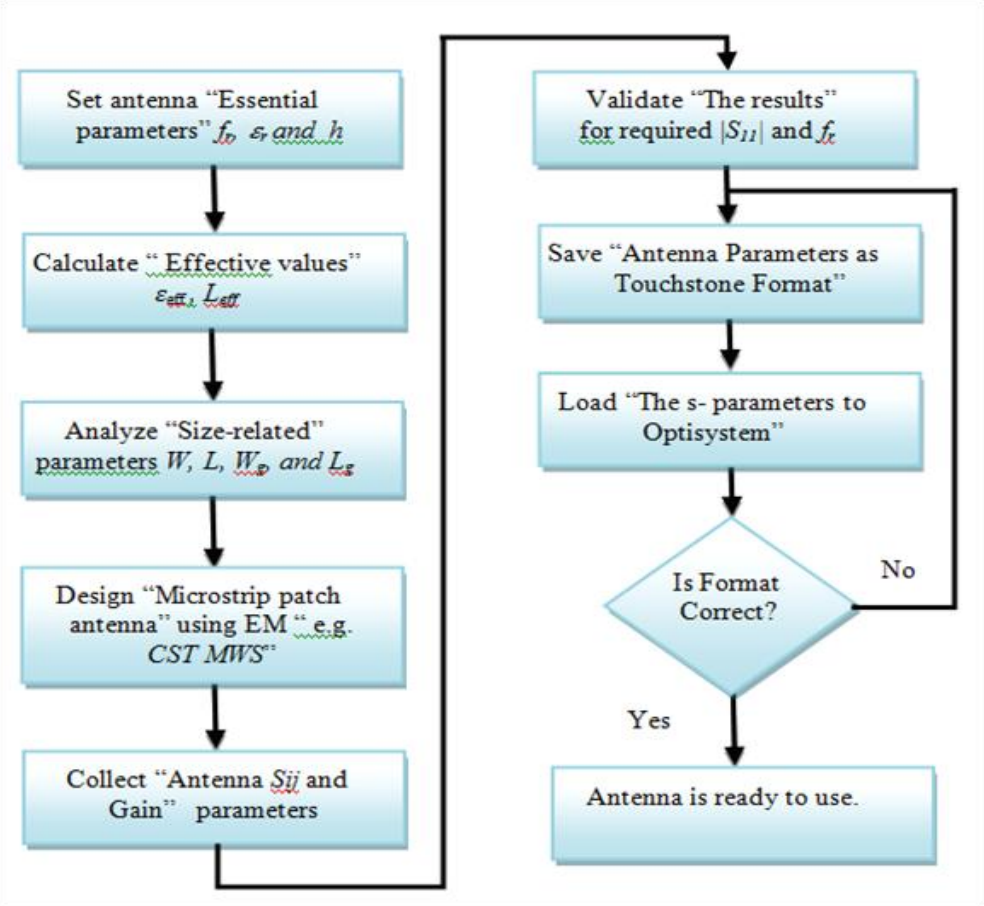

Figure 3.9. Flowchart of the proposed microstrip patch antenna design and installation Procedure

3.4 Free Space Path Loss and Link Budget Calculations

Before designing a radio system, we should understand all the channel characteristics that could affect the performance of the system. The first characteristic is the free space path loss (FSPL). FSPL is defined as the loss of the signal strength of an electromagnetic wave that results from a line of sight (LOS) path through free space [79].

3.4.1 Free space path loss

To predict the radio signal strengths that may be expected in a radio system, the free space path loss must be considered. The signal travels from one point to another with

a reduction of strength. This is because the transmitting and receiving antennas are separated by distance (*d*). The free space path loss is a function of the antenna's operating frequency and the distance between them. The free-space loss characteristic of an RF signal can be explained by Friis transmission equation [80]. The simple form of the Friis transmission equation was derived in 1945 as follows:

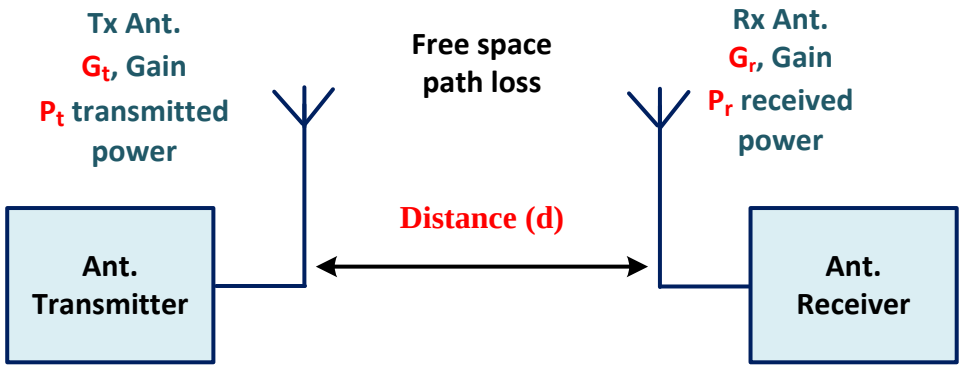

Figure 3.10. Free space Model

Consider figure 3.10. This figure illustrates a transmitting antenna $\boldsymbol{T_x}$ and a receiving antenna $\boldsymbol{R_x}$. These two antennas operate at a wavelength of $\boldsymbol{\lambda}$ and they are separated by distance ***d***. The high frequency energy that is emitted by an isotropic radiator would propagate uniformly in all directions. The surface areas with the same power density *P* then form spheres ($A = 4\pi R^2$) around the radiator. The same quantity of energy spreads out on an incremented spherical surface at an incremented spherical radius. That means, the power density on the surface of a sphere is inversely proportional to the surface area *A* (or the square of the radius *R*) of the sphere.

The expression for the FSPL, in fact, encapsulates two effects. FSPL is proportional to the distance squared, d^2, between both antennas, and it is proportional to the f^2, the frequency of the radio signal. First, the spreading out of electromagnetic energy in free space is determined by the inverse square law, that is,

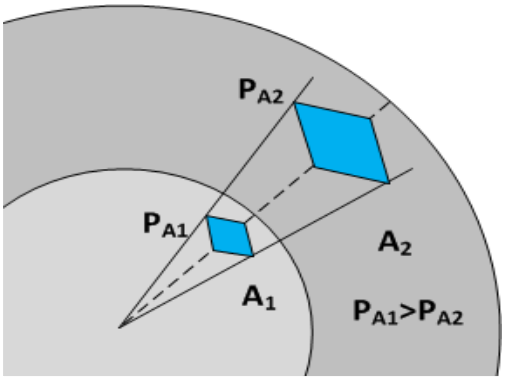

Figure 3.11. Power density and radiation of the power around the surface

Power density *P* can be expressed by:

$$P = \frac{P_t}{4\pi d^2} \quad . \tag{3.16}$$

The received power is given by:

$$P_r = P.A_{eff} \tag{3.17}$$

where, A_{eff} is the effective aperture of the antenna.

$$P_r = \frac{P_t}{4\pi d^2}.G_t.A_{eff} \tag{3.18}$$

And

$$A_{eff} = \frac{\lambda^2}{4\pi}.G_r \tag{3.19}$$

From equations 3.18 and 3.19 we can express the received power P_r at the receiving antenna *Rx*. This equation is called the Friis transmission formula.

$$\frac{P_r}{P_t} = G_t . G_r (\frac{\lambda}{4\pi d})^2 \quad (3.20)$$

Where P_r is the power received by the receiving antenna; P_t is the power input to the transmitting antenna; G_t and G_r are the antenna gains of the transmitting and receiving antennas, respectively; λ is the wavelength, and d is the distance between the transmitting and receiving antennas. This equation shows that the received power is inversely proportional to the frequency.

However, propagation loss gets larger with an increase of wireless transmission distance at higher frequencies. For example, the 10 m and 30 m free-space transmission would induce about 60 dB and 70 dB losses respectively for a 2.4-GHz RF signal. The expression for FSPL mainly contains two effects. However, FSPL is proportional to the d^2 between both antennas, and it is also proportional to the f^2 of the radio signal. The FSPL can be obtained from the Friis transmission formula in equation (3.20) as follows:

$$FSPL = \left(\frac{4.\pi.d}{\lambda}\right)^2 \quad (3.21)$$

where λ is the radio signal wavelength at operating frequency of 2.4 GHz ($\lambda = c/f$) and d is the distance between the transmitting antenna and the receiving antenna. After replacing λ with speed of light and frequency in the free space, the path loss formula of equation (3.22) becomes:

$$FSPL=\left(\frac{4\pi df}{c}\right)^2 \quad (3.23)$$

Or FSPL in decibels equation (3.20) becomes:

$$FSPL(dB) = 10log_{10}(\frac{4\pi df}{c})^2$$

$$= 20log_{10}(\frac{4\pi df}{c})$$

$$= 20\log_{10}(d)+20\log_{10}(f)+20\log_{10}\left(\frac{4\pi}{c}\right) \quad (3.24)$$

It is a typical for radio applications to find *d measured* in km and *f* in MHz, and then the FSPL equation (3.24) becomes:

$$FSPL(dB)=20Log(d) + 20Log(f) + 32.44 \quad (3.25)$$

In equations (3.25), the transmitting and receiving antenna gains G_{tx} and G_{rt}, respectively, are not included, and they are considered unity for both antennas. Then the general equation for calculating the FSPL, including both antenna gains is as follows:

$$FSPL(dB)= 20\ Log10(d)+20\ Log10(f)+32.44-Gtx-Grx. \quad (3.26)$$

FSPL calculations are often used to help predict RF signal strength in an antenna system. Loss increases with distance at a fixed operating frequency as presented in equation (3.25) and illustrated in figure 3.12. Hence, understanding the FSPL is an essential parameter for engineers dealing with RF communications systems.

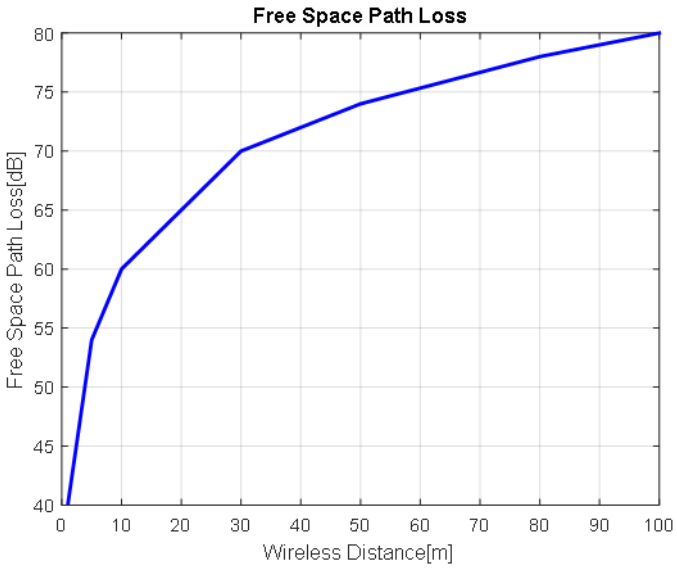

Figure 3.12. free space loss vs. distance for 2.4 GHz signals

3.4.2 RF link budget calculation

Calculating an RF link budget is very important to predicting and estimating the range and link margin. The theoretical analysis of any system performance is based on predicting a value for the signal-to-noise ratio (*SNR*) at the receiver. Therefore, it is necessary to calculate the actual received SNR when evaluating the actual system performance in a certain application [81]. This calculation requires a link budget, which means a careful accounting of the various terms in the following equation for receiving SNR:

$$\text{SNR}=\frac{Signal\ power\ in\ watt}{Noise\ power\ in\ watt} \tag{3.27}$$

SNR expressed in dB becomes:

$$\text{SNR (dB)= Received signal power (dBm) – receiver noise power (dBm)} \tag{3.28}$$

Where,

$$\text{Received signal power (dBm) =Transmitted power (dBm) +Link gains (dB) -Link losses (dB).} \tag{3.29}$$

A customized spreadsheet is used to design the radio frequency link as illustrated in Appendix C.

3.5 Summary

This chapter has been devoted to the description of basic concepts of a microstrip patch antenna and FSPL link budget. In Section 3.2, the microstrip patch antenna method of analysis and design were provided. Also, the antenna's actual dimensions and results were obtained using Matlab and CST simulations. The microstrip patch antenna return loss R_L and the gain were calculated. The transmitting and receiving antenna scattering

parameter files were organized in Touchstone format and are listed in Appendix A. In section 3.3, the passive microstrip patch antenna was upgraded by adding a low-power RF amplifier and a bandpass filter to become an active antenna for coverage extension. The FSPL equations and link budget calculations were presented in section 3.4. In the next chapter, the designed antenna parameters are used in different models and simulations.

Chapter Four: Chapter Four: Optical OFDM Based W-LAN System: Modeling, and Simulations

4.1 Introduction

Deployment of OFDM in optical communications has grown rapidly and is attracting more attention. Numerous applications in this subject are now available. Two scenarios have been proposed for the optical OFDM systems [7], [51]: A direct–detection optical OFDM (DD-OOFDM) and coherent detection optical OFDM (CO-OFDM). The DD-OOFDM type consists of a simpler receiver which makes it more cost-effective, and the CO-OFDM type is widely used for long-haul optical communications. Recently, OFDM has also been implemented in optical communications to overcome wireless coverage area deficiencies [8]. Due to the cost factor of the optical access network, it is necessary to utilize a low-cost optical front end. Therefore, for low-cost optics, the intensity-modulation direct detection (IMDD) technique is unrivaled and either direct modulation or external modulation of a laser source can be utilized. Directly modulated lasers (DMLs) are preferred for their lowest cost solution. A normal photodiode pin is used for optical to electric conversion purposes. However, the combination of optical and wireless systems can provide better service in densely populated areas such as airports, shopping centers, office buildings dead-zone areas and tunnels. Passive microstrip patch antennas have a limited radiation distance that is considered a major drawback in wireless

communication networks. The active antenna concept has been in use in microwave engineering for some years [11]. Typically, RF signal transmission for fiber optics is considered over SMFs. Recently, MMFs have increasingly been applied to *short distance* applications as an alternative to single mode ones. However, this attraction comes from MMFs existence in modern buildings and campuses. To effectively implement the microstrip patch antenna parameters described in chapter 3, such as S-parameters and the antenna gain in an optical-wireless communication link, Optisystem tools are used. These quantities can be modified as a Touchstone format to represent the proposed antenna to produce S2P in the Optisystem.

The rest of the chapter is organized as follows: in section 2, the conventional optical based W-LAN model using a QAM modulation technique is presented. In section 3, the proposed optical OFDM based W-LAN system configuration using a direct modulation technique is outlined and covered in detail. In section 4, the proposed optical OFDM based W-LAN system configurations using an external modulation technique for both downlink and uplink are explored.

4.2 Conventional Optical Based W-LAN Signal using QAM Modulator.

The purpose of this model is to carry a modulated W-LAN signal over an optical fiber and distribute it wirelessly using the microstrip patch antenna transmitter ***Tx***. At the receiver, the signal is received and demodulated using a QAM demodulator. An optical fiber length and free space distance are the main variables in this model.

4.2.1 System model and parameters

The system model is illustrated in figure 4.1. The block diagram of a conventional optical wireless consists of a digital signal transmitter, optical link components, identical microstrip patch antennas separated by a free space link and a digital signal receiver.

First, the blocks are built using Optisystem communication tools and for the wireless part, Touchstone file format specifications are used for implementing the designed patch antenna scattering parameters |Sij| in the two port component S2P. The main variable parameters are the fiber length and the free space path between the microstrip patch antennas. The SMF optical fiber length varies from 1 km to 80 km without any optical amplification component. The distance between the antennas (in term of decibels) varies from 40 dB to 80 dB. The system blocks are discussed in details as follows:

4.2.1.1 System transmitter

On the transmitter side, the stream of bits is generated using a pseudo-random bit sequence generator (PRBS). The PRBS generates a sequence with a length of (2^k-1), where k is the PRBS order and can be calculated by:

$$K=\log(\text{sequence length})/\log(2) \quad (4.1)$$

The generation of the bit stream is based on Mark probability, where the probability of ones in the sequence is equal to the probability of zeros in the sequence which is 0.5. This means the number of ones generated is equal to the number of zeros. However, the order of the PRBS generator depends on the bit sequence length as it is shown in the equation (4.1).

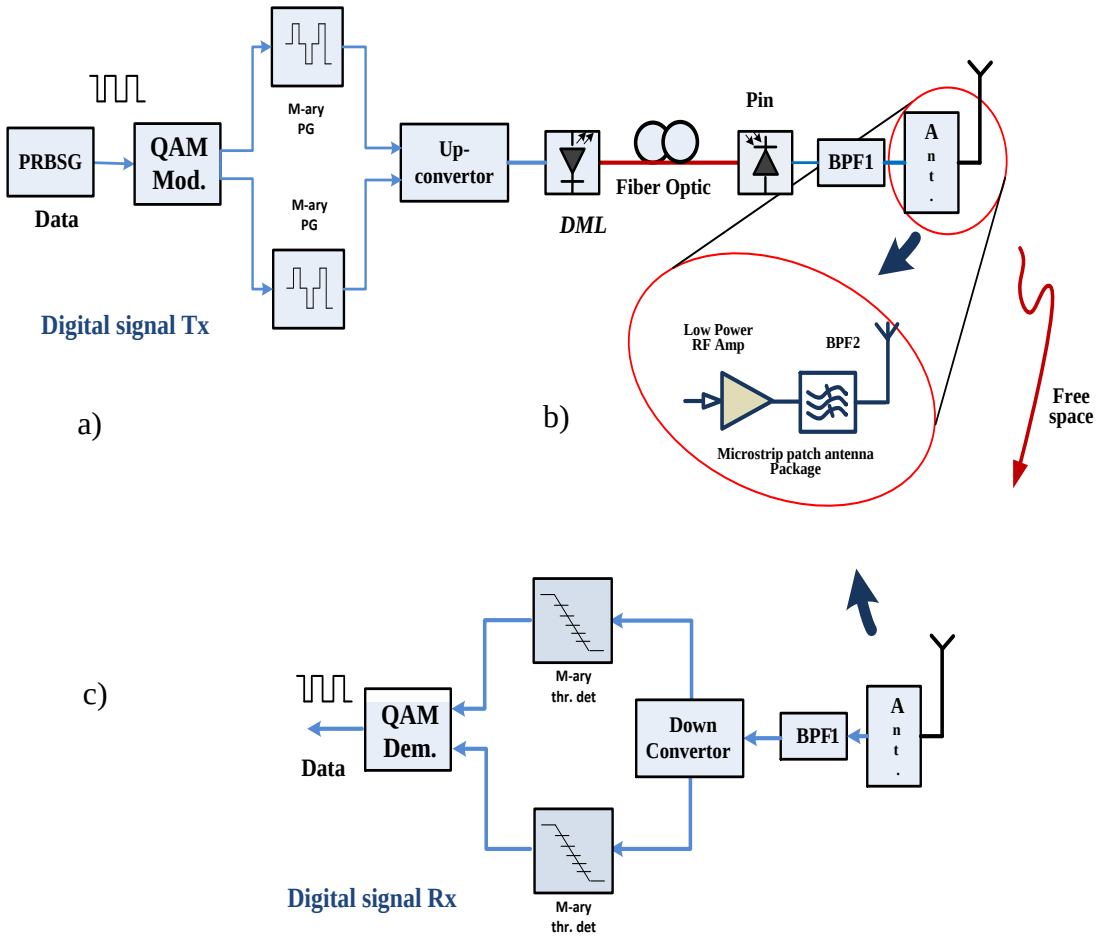

Figure 4.1. Block diagram of the conventional optical system using a QAM modulator a) Digital system transmitter. b) Active microstrip patch antenna.
c) Digital system receiver.

The received sequence of bits from the PRBS generator with an order of k are mapped to the M-QAM constellation, where $M=2^n$, and n is the number of bits per

symbol. For example, if the number of bits n=2, then the M=4 and we get 4-QAM, 16-QAM for *n*=4, and 64-QAM for *n*=6. At the QAM output, the bit sequence is split into two parallel subsequences. The M-ary pulse generator generates multilevel pulses according to the M-ary signal input. In the case of 4-QAM, there are two levels (1 and -1) of pulses generated, and each can be transmitted in two quadrature carriers.

The pulses are received at the Quadrature Modulator (QM), and a QM implements a quadrature analog amplitude modulator. The output signal is modulated according to equation (4.2) [97]:

$$v_{out}(t) = G[I(t)\cos(2\pi f_c t + \emptyset_c) - Q(t)\sin(2\pi f_c t + \emptyset_c)] + b \qquad (4.2)$$

where *I* and *Q* are the input electrical signals; *G* is the gain; *b* is the bias, and in this simulation, it is set to 1. The radio frequency f_C is set to 2.4 GHz, which is the same frequency of the microstrip antenna operating frequency and $\emptyset_c$ is the carrier phase.

4.2.1.2 Optical link

For low-cost optics, the DML is utilized for direct modulation as a laser source, and an *InGaAs* pin photodetector type is used for direct detection and an *SMF* for a fiber optic link. In this section, we describe the analog optical link components in details.

In the analog optical link, the *DML* is adopted as an optical source that operates at a wavelength of 1550 *nm* and has -130 *dBm/Hz RIN* and a slope efficiency of 0.2 *W/A*. A SMF is the only fiber used in this section. The used standard SMF has a 9/125 micron and 0.2 *dB/km* attenuation. SMF also has a dispersion of 16.75 *ps/nm/km* and operates at a wavelength of 1550 *nm*. In optical wireless communications where small size, low-cost

components are needed, the use of optical amplifiers such as EDFAs or semiconductor optical amplifiers (SOA) is not highly recommended [14]. The used SMF parameters are summarized in Table 4.1.

Table 4.1 SMF parameters

Parameter Name	Parameter Value	Symbol
Fiber length(L)	1 - 80	*Km*
Wavelength (λ)	1.55	*Mm*
Attenuation (α)	0.2	*dB/km*
Dispersion(CD)	16.75	*ps/nm/km*
Dispersion Slop	0.075	$Ps/nm^2/km$
Differential group delay	0.2	*Ps/km*

The function of the photodetector in an optical link is to receive the output optical power of the fiber for detection and convert it to electrical power in terms of electrical current. The performance of a photodiode may be characterized by its responsivity *R*. This parameter is quite useful since it specifies the photocurrent generated per unit optical power.

Table 4.2: Generic operating parameters of Si, Ge, and InGaAs pin Photodiodes

Parameters	***Symbol***	***Unit***	***Si***	***Ge***	***InGaAs***
Wavelength	Λ	*Nm*	*400-1100*	*800-1650*	*1100-1700*
Responsivity	$\Re$	*A/W*	*0.4-0.6*	*0.4-0.5*	*0.75-0.95*
Dark current	I_D	*Na*	*1-10*	*50-500*	*0.5-2.0*
Rise time	τ_r	*Ns*	*0.5-1*	*0.1-0.5*	*0.05-0.5*
Bandwidth	*B*	*GHz*	*0.3-0.7*	*0.5-3*	*1-2*
Bias voltage	V_B	*V*	*5*	*5-10*	*5*

In this study, we conducted our experiments with an *InGaAs pin* photodetector type with a typical responsivity value of 0.8 *A/W* at 1550 nm and a dark current value of 10 *nA* as obtained from Table 4.2. The photodetector has a thermal noise value of $4x10^{-21}$ *W/Hz*.

4.2.1.3 Wireless system link

The wireless link consists of transmitting and receiving microstrip patch antennas as in figure 4.1b and free space link with a variable distance "*d".* Both the transmitting and receiving antennas are identical, where each antenna is a standard inset-fed microstrip operating at 2.4 GHz with an omnidirectional radiation pattern. Also, the passive antenna is upgraded to become an active antenna by integration with a package of components as mentioned in chapter 3. The package consists of a band-pass filter and an RF low power amplifier. The band-pass filter has a bandwidth of 70 MHz, which is enough to accommodate the radio signal at that point, while the RF amplifier data is obtained from the SKY65016-70LF data sheet. The used RF amplifier is a general purpose, broadband amplifier. The device is fabricated from the Skyworks InGaP HBT process and has a small signal gain about 20 dB at 2 GHz. It also has a high 3rd order output intercept point (OIP3) of + 27 dBm typical and a 1 dB output compression point OP1dB of +14 dBm at 2GHz too. The device's 50 Ω input and output impedance allow it to be easily cascaded without external impedance matching networks. The typical –3 dB bandwidth of the SKY65016-70LF is 0.1 to 3.0 GHz. The amplifier's operating temperature is in the range of (-40 ^{o}C to +85 ^{o}C). This device has 4-pins and 1.5x4.0 mm

package size. The noise figure (NF) of the RF amplifier is 4.8 dB and noise power of -170 dBm is included [19].

4.2.1.4 System receiver

At the receiving side, the RF signal is received by the receiving antenna as shown in figure 4.1c. The signal is filtered, amplified, and down-converted using the quadrature modulator (QD). The received data from QD passes through an M-ray threshold detector. Then the M-ray detector compares the electrical signal at a user-defined decision instant with a list of threshold levels. The comparison generates an index used to generate the output amplitudes. For example, if the signal input has a value of -0.8, the output level will be -1, since -0.8 is between -1 and 1 and the decision instant, basically, is 0.5 bit for two-level output amplitudes. Then the QAM sequence decoder decodes two parallel QAM M-ary symbol sequences to a binary signal, and the transmitted data sequences are recovered back and received by the end user.

4.2.2 Simulation results and discussion

To validate that the design of the transmitting and receiving antennas is working properly at 2.4 GHz, the simulations ran for different frequencies around the central frequency 2.4 GHz to see where the maximum power reception falls. We can clearly see from figure 4.2 that the maximum received power is obtained at the radio center frequency of 2.4 GHz. This indicates that the reception of the signal from the transmitting antenna is at its maximum. Different visualizers are used for measuring power, spectrum, OSNR, SNR, BER and received constellations as shown in the appendices C1, C2 and C3.

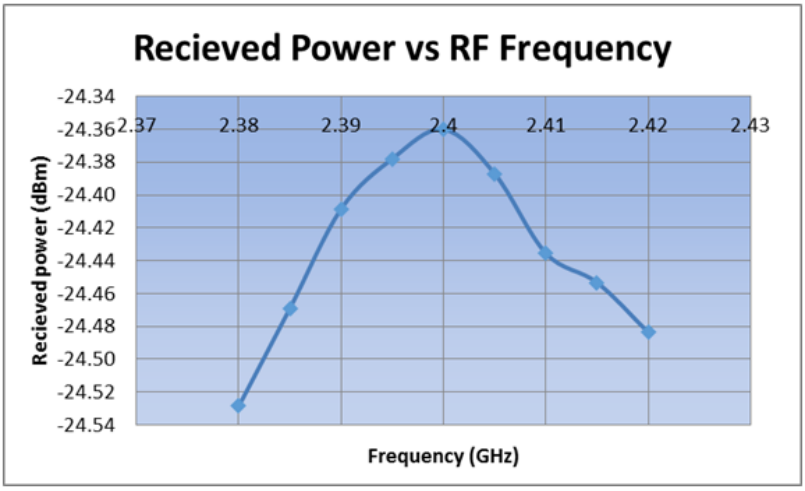

Figure 4.2. Antenna-received power vs. RF frequency.

In this section, all the simulations have fixed global parameters, such as bit rate and the number of mapped bits per symbol. The received RF signal by the laser diode DML is launched to the optical fiber with a power value of 1 mw (0 dBm). The obtained results and comparisons between the passive and active microstrip antennas are presented. Also, the system performance in term of BER, S/N, and constellation signals is discussed.

Figure 4.3 shows the EIRP, S/N and the received noise signal from the active antenna. From figure 4.3, we can observe that the EIRP decreases with an increase in fiber length. Also, the effect of the wireless link on receiving power is more noticeable. The active antenna SNR is still high enough and is not highly affected by the short distance of 60 dB in the wireless link.

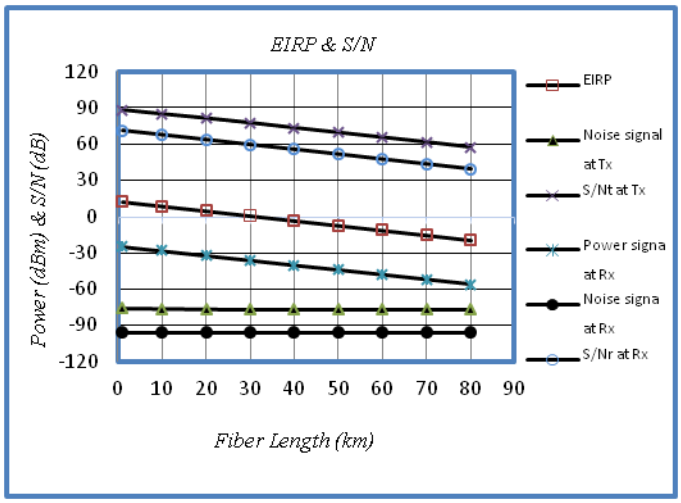

Figure 4.3. Comparison of the signal power and S/N vs. the fiber length of the patch antenna output, *FSL=60 dB [38]*

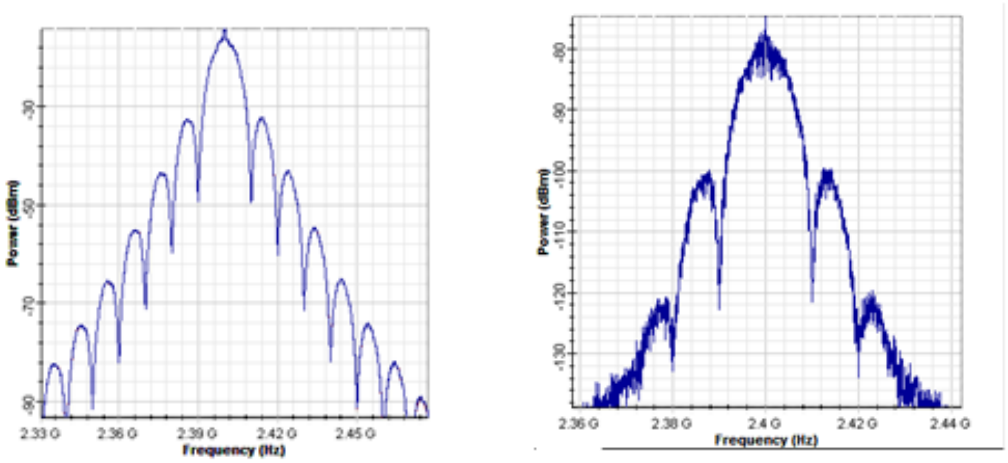

a) b)

Figure 4.4 a) The spectrum of the signal at the transmitter b) the spectrum of the signal after traveling 50 km over the SMF and 60 dB in free space propagation.

Figure 4.4 illustrates the signal spectrum at the transmitter side and the received signal at the receiver after traveling through a 50 km SMF optical link and 60 dB free

space propagation. From figure 4.4, we can see the degradation of the signal because of the FSP attenuation.

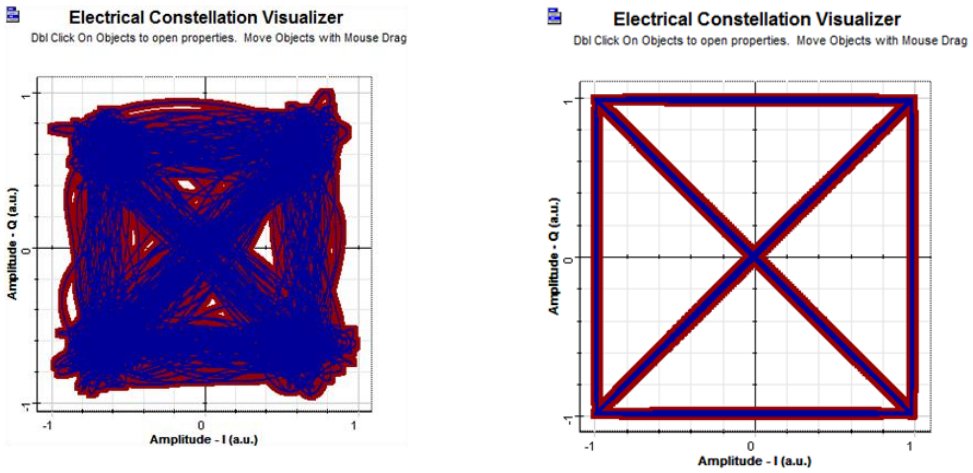

a) b)

Figure 4.5. Constellation diagram of receiving signal after attenuation by FSL=60 dB and 50 km in SMF using a) Passive patch antenna b) Active patch antenna.

Figure 4.5 represents the differences between both the received signal constellations in polar form. Figure 4.5 represents the receiving signal constellations when the passive antenna is used, while figure 4.5b illustrates the receiving signal constellations when the active antenna is utilized. In conclusion, the results show the advantage of utilizing the active microstrip antenna in the proposed system compared to the passive one.

4.3 Optical OFDM Based W-LAN System

This section covers an optical OFDM down-link from the signal generated at the BRPS generator through the reception of the signal at the end user. However, the difference between the previous modeling system in section 4.2 and this system is that

here, the digital signal is processed using the OFDM as a multicarrier modulation technique instead of QAM scheme only as was done in the conventional optical system.

The results of this section were published in "Kenshil, S., Rashwan, G., & Matin, M. (2017). Analysis of optical OFDM-based W-LAN. In *Computing and Communication Workshop and Conference (CCWC), 2017 IEEE 7th Annual* (pp. 1-5)".

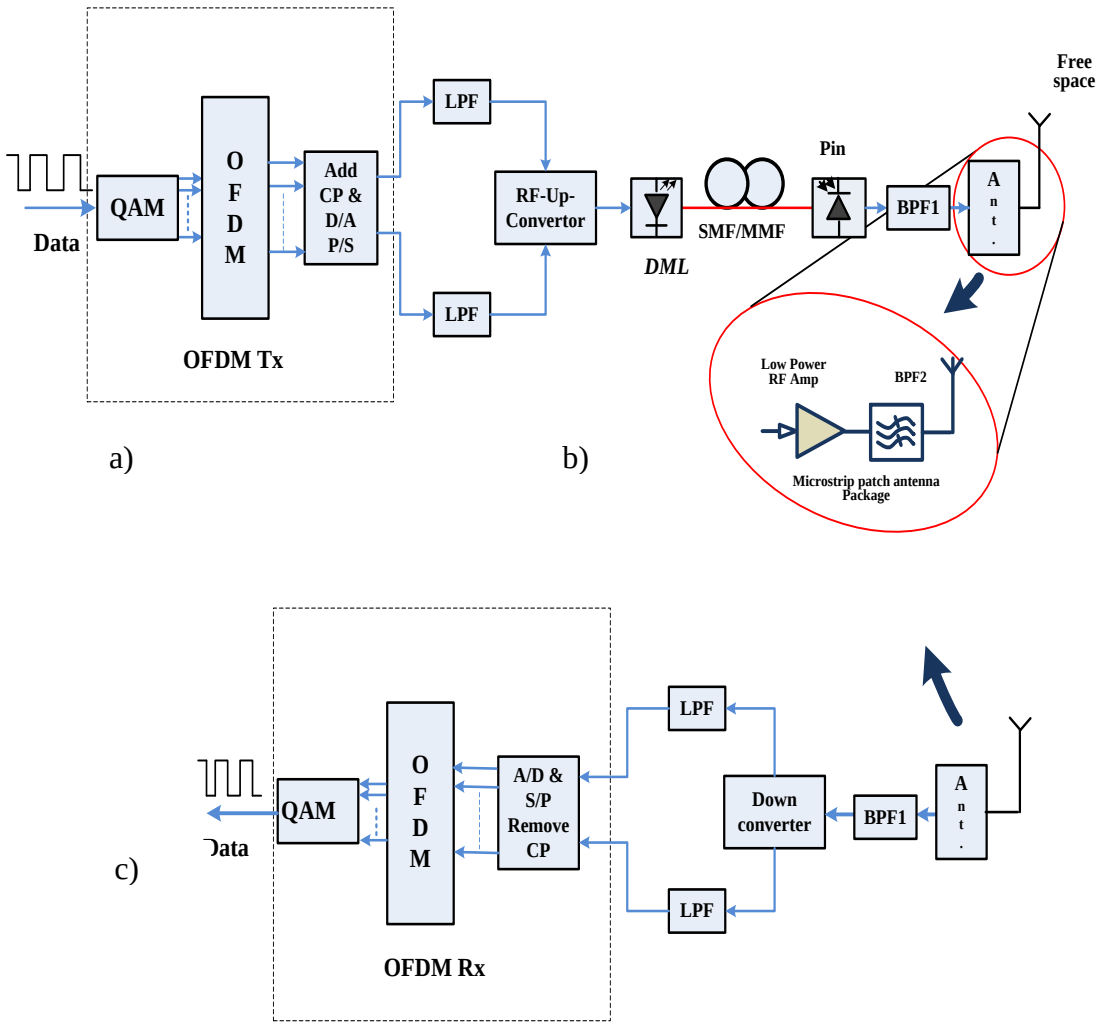

Figure 4.6. Downlink block diagram of an optical OFDM based W-LAN system. a) Optical OFDM transmitter. b) Microstrip patch antenna. c) OFDM receiver.

4.3.1 System model and parameters

Figure 4.6 shows the typical block diagram of an integrated optical OFDM wireless link. This block diagram consists of an OFDM transmitter and receiver, optical components and two identical microstrip patch antennas separated by a modeled FSPL by a distance *d* as shown in figure 4.6. First, at the OFDM transmitter side, streams of data are generated using the PRBS generator in the same way for the conventional optical block diagram. Figure 4.7 illustrates a sketch diagram showing the OFDM signal processing steps at different stages of the blocks.

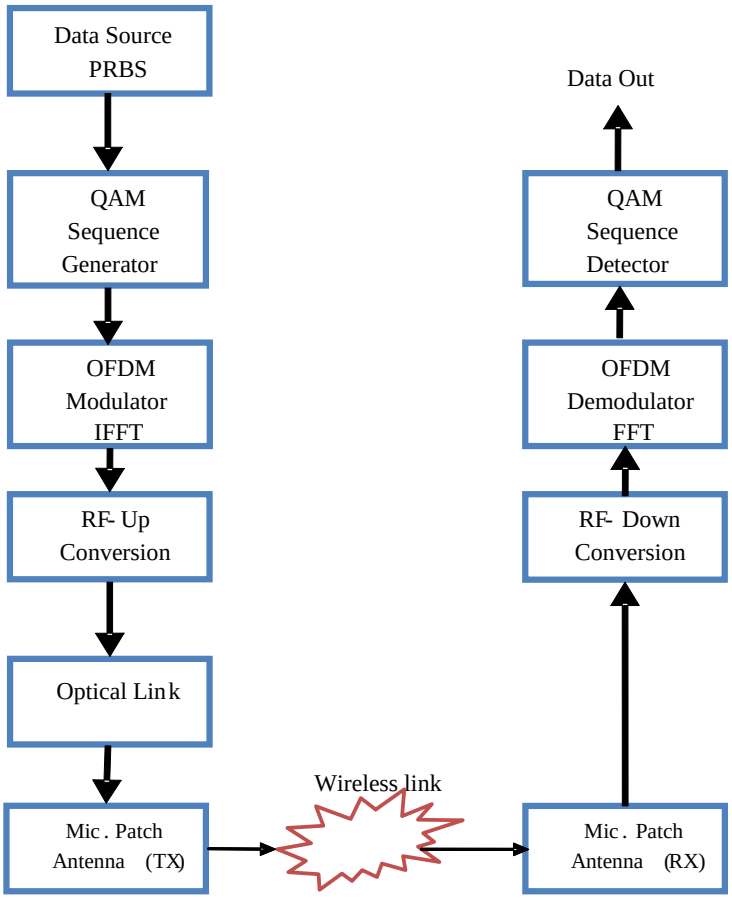

Figure 4.7. Sketch diagram showing the stages of the OFDM signal processing

The PRBS generates a sequence with a length of (2^{11}-1). Then, the received sequence of bits from the PRBS is mapped to the 4-QAM constellations, which are two bits per symbol. These symbols are converted into frames of *N* parallel rows which is 48 subcarriers carrying data for a W-LAN system. Also, four pilot subcarriers are added to the string of each frame to make a total of 52 subcarriers. The main purpose of the pilot is used at the receiver for synchronization and channel equalization if needed. Then the stream of data is received at the OFDM transmitter in parallel rows. The OFDM transmitter and receiver block diagrams are shown in figure 4.8. As is illustrated in figure 4.8, the used modulation scheme is a QAM scheme for all the simulations. The 4-QAM symbols are mapped into 52 orthogonal subcarriers defined in the OFDM to form a vector fit for inverse fast Fourier transform (IFFT) input.

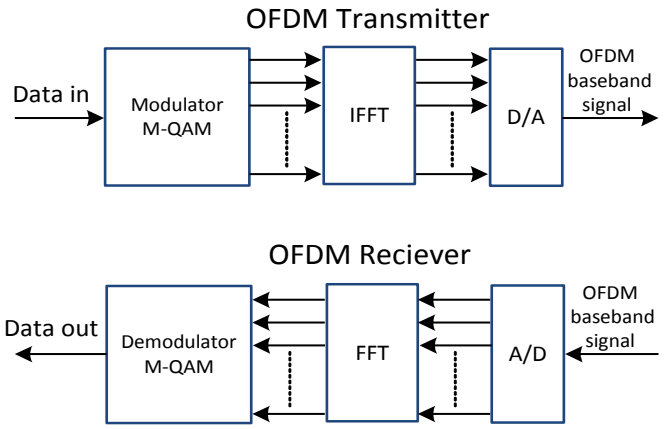

Figure 4.8. OFDM transmitter and receiver blocks [38]

The IFFT and FFT are the functions, which distinguish OFDM from single carrier systems. IFFT, a fast algorithm for computing DFT, can further reduce the number of arithmetic operations from N2 to *NlogN*, where N is the size of the FFT. IFFT is also

employed to convert the complex data in the frequency domain into a stream of data in the time domain at the OFDM transmitter's side, while FFT is the opposite operation achieved at the receiver side.

We consider the complex vector $\boldsymbol{X}$ at the input to the IFFT [7],

Where, $\boldsymbol{X} = [X_0 \ X_1 X_2 \ \ldots X_{N-1}]^{\boldsymbol{T}}$.

The vector has a length *N* where *N* is the size of the IFFT. For W-LAN, 64-FFT points are applied as shown in Table 4.3. Each of the elements of *X* represents the data to be carried on the corresponding subcarrier. Usually, QAM modulation is used in OFDM, so each of the elements of *X* is a complex number representing a particular QAM constellation point. The output of the IFFT is the complex vector x,

Where, $\boldsymbol{x} = [x_0 \ x_1 x \ \ldots x_{N-1}]^{\boldsymbol{T}}$.

The general mathematical expression for a transmitted OFDM signal is expressed as in equation (4.3):

$$x_m = \frac{1}{\sqrt{N}} \sum_{k=0}^{N-1} X_k \left(e^{\frac{j2\pi km}{N}}\right), \ for \ 0 \le m \le N-1 \qquad (4.3)$$

Where X_k is the data symbols at k_{th} subcarrier, and N is the size of the IFFT and FFT. The N_{SC} is the number of OFDM subcarriers and $N_{SC} \le N$, where all the subcarriers are equally spaced by Δf as shown in figure 4.9.

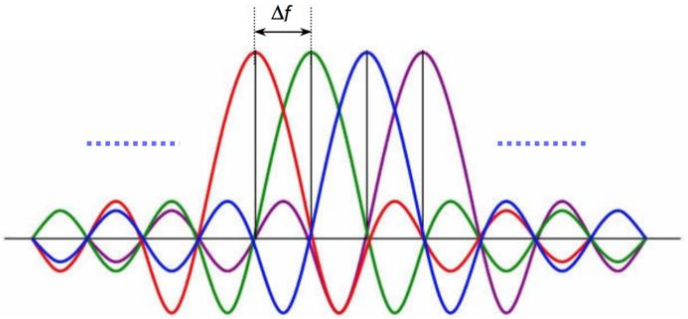

Figure 4.9 OFDM subcarriers equally spaced by Δf to preserve orthogonal

To avoid ICI caused by multipath channels, the *CP* is a copy of a part of the OFDM symbol added to the end of the symbol and used to separate adjacent OFDM symbols instead of the null guard. Then at the receiver before the FFT block, this *CP* will be removed. Throughout the simulations, the *CP* period has a fixed length which is ¼ of the OFDM symbol observation period. Table 4.3 provides the used parameters in the system based on IEEE 802.11 standard for W-LAN.

Table 4.3 W-LAN system parameters for DD-OOFDM model

Parameters	**Value**
N_{SD}: Number of Data subcarriers	48 Subcarrier
N_{SP}: Number of Pilot subcarriers	4 Pilot
N_{ST}: Total number of subcarriers	52 (N_{SD}+N_{SP})
N_{FFT}: Number of FFT points	64 points
Δ_F: Subcarrier frequency spacing	0.3125 MHz (=20 MHz/64)
T_{FFT}: IFFT/FFT period	3.2 μs ($1/\Delta_F$)

Following the insertion of the *CP* for every OFDM symbol, a digital to analog converter (D/C) is employed to OFDM signal before the conversion to RF signal. In addition, a low pass cosine roll off filter with a roll factor of $0 \leq r_p \leq 1$ is used, and it is observed that when r_p =0.2 provides better results. Then the data passes through a parallel-to-series convertor. The up-conversion is used in the quadrature modulator (*QM*) to modulate the OFDM baseband signal and generate the analog waveform at 2.4 GHz radio carrier frequency. The signal information will modulate the optical light before being launched into an optical link.

- **Low pass cosine-roll off filter.**

The LP cosine roll off filter transfer function [36]:

$$H(f) = \begin{cases} \alpha & (|f| < f_1) \\ \sqrt{0.5.\alpha^2\left[1 + cos\left(\frac{|f| - f_1}{r_P.\Delta f_{FWHM}}.\pi\right)\right]} & (f_1 \leq |f| < f_2) \\ 0 & (f_2 \leq |f|) \end{cases} \qquad (4.4)$$

Where α is the parameter insertion loss; f_c is the filter cutoff frequency, and r_p is the parameter roll off factor. The parameters f_1 and f_2 are:

$f_1 = 1 - r_p . f_c \quad (0 \leq r_p \leq 1)$

$f_2 = 1 + r_p . f_c \quad (0 \leq r_p \leq 1)$

- **Optical link components.**

In this analog optical link, we use the same optical parameters that were used in section 4.2. The *DML* is adopted as an optical source that operates at a wavelength of 1550 *nm* and has -130 *dBm/Hz RIN* and a slope efficiency of 0.2 *W/A*.

Two optical fiber types are used: SMF and MMF fiber optic. SMFs are used mainly for a long distance application which has a 9/125 micron, and its parameters are listed in Table 4.1. MMF is commonly employed for short distance applications such as in-building for LANs and has commonly either 62.5/125 or 50/125 micron standards and MMF can operate at either 1310 nm or 1550 nm wavelengths.

An *InGaAs pin* photodetector type with a typical responsivity value of 1 *A/W* at 1550 nm and a dark current value of 10 *nA* as obtained from figure 4.10 is employed. Also, the photodetector has a thermal noise value of $4\text{x}10^{-21}$ *W/Hz*. The photodiode responsivity *R* can be calculated as follows:

$$\eta = \frac{\#\text{ of electron - hole photogenerated pairs}}{\#\text{ of incident photons}} \tag{4.5}$$

$$\eta = \frac{I_P / q}{P_0 / h\nu} \tag{4.6}$$

$$\Re = \frac{I_P}{P_0} = \frac{\eta q}{h\nu} \quad \text{[A/W]} \tag{4.7}$$

Where η is the quantum efficiency, I_P is the photocurrent, and P_O is the incident optical power. The relationship between the *InGaAs* p-i-n photodetector responsivity and the wavelength is illustrated in figure 4.3.7.

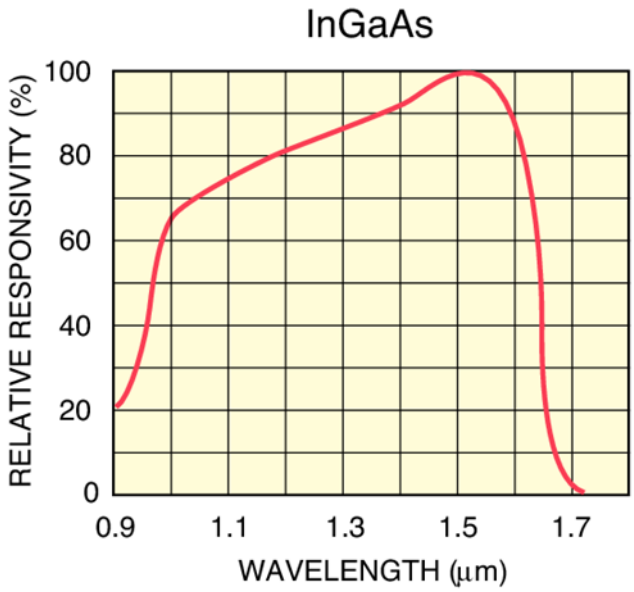

Figure 4.10. Relative responsivity vs wavelength for *In GaAs* p-i-n photodiode

- **The wireless link**

Figure 4.11 illustrates the two identical microstrip patch antennas separated with a free space distance (*d*) that was used with the same functionality and parameters as in section 4.2.

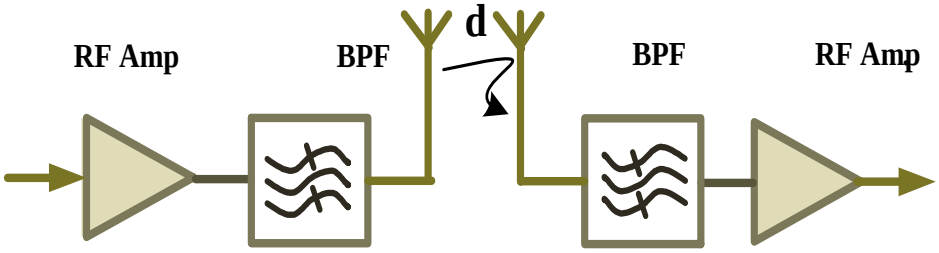

Figure 4.11. Illustrates the two identical active microstrip patch antennas separated by a free space distance (*d*).

At the receiver side, the signal is filtered and amplified and down converted using the quadrature modulator (QDem). Then the signal is filtered with a low-pass filter and signal converted to digital signal again using an analog-to-digital converter (ADC). The *CP* is removed and the received information symbol for each subcarrier is extracted by performing an *FFT* with the same N_{FFT} points as seen in equation (4.8)

$$Y(k) = \frac{1}{\sqrt{N}} \sum_{k=0}^{N-1} y_m \left(e^{\frac{-j2\pi km}{N}}\right), \ for \ 0 \leq k \leq N-1 \tag{4.8}$$

At the final stage, these extracted OFDM symbols are demodulated using a QAM demodulator as illustrated in figure 4.6.

4.3.5 Simulation results

All the blocks were built using Optisystem communication tools. The wireless part, Touchstone file format specifications for implementing the antenna scattering parameters |Sij| in the two ports component *S2P* were used. Specifically, two main variable parameters were used for the simulations besides the launched optical power, the fiber length and the free space path between the microstrip patch antennas. The SMF optical fiber length varied from 1 km up to 80 km without any optical amplification component. Also, the distance between the antennas in term of decibels varied from 40 dB up to 80 dB.

In this section, we demonstrate some of the obtained results and comparisons between active and passive microstrip antennas. For example, the EIRP, signal and noise power values for both antennas with variable fiber lengths and free space losses are

presented. Also, the system performance in terms of, OSNR, SNR, BER and constellation signals is discussed.

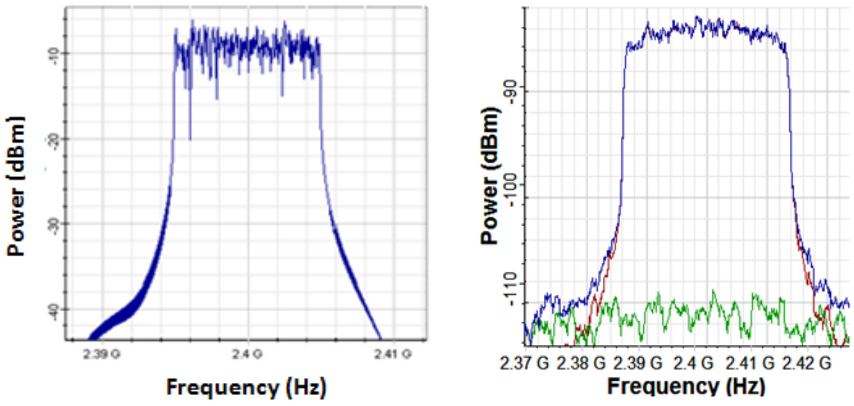

a) b)

Figure 4.12 a) Transmitted OFDM signal b) Received OFDM signal after 50 km fiber length and 70 dB path loss.

Figure 4.12 illustrates the transmitted and received OFDM signal over the designed integrated optical wireless link. The signal is received after traveling 50 km through an optical SMF, and it has retained its shape even after 30 m distance in free space propagation.

Figure 4.13 shows the distorted transmitted signal and the effect of phase noise on the constellation signals. This figure shows the received electrical-signal constellations without phase equalization. The unequalized constellations show that the phases of the received electrical subcarriers are spread over a circle due to the fiber dispersion inducing the frequency dependent phase shift. A compensation system or an optical component should be selected carefully to avoid any extra noise on the transmitted signals.

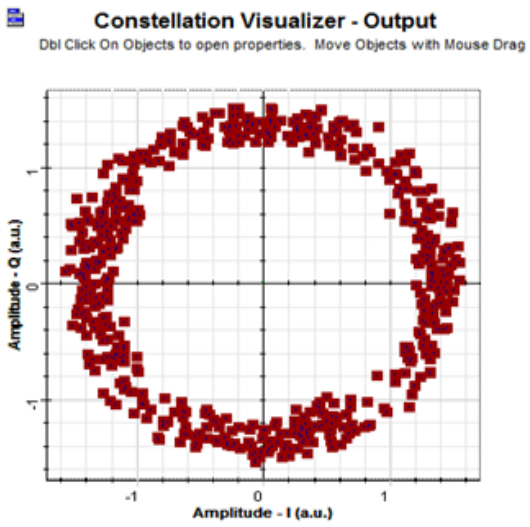

Figure 4.13. The effect of phase noise on transmitted signal

Even though there is no overlap between the two OFDM symbols, which means the ISI cannot exist, there exists a phase offset that is proportional to the STO forcing the signal constellation to be rotated around the origin.

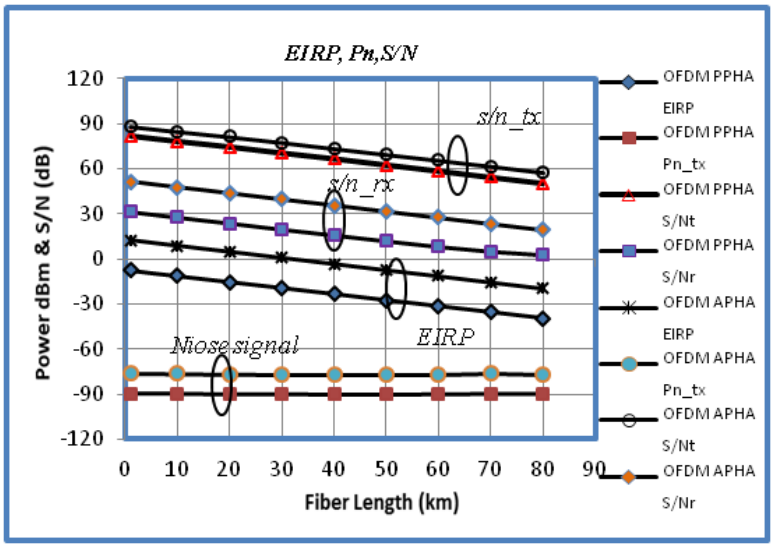

Figure 4.14. A comparison between the OFDM active and passive patch antennas in terms of transmitting power and noise and S/N and received S/N at FSL 60 dB for different fiber lengths.

Figure 4.14 illustrates the transmitted power and received power at different fiber lengths with FSL of 60 dB. From figure 4.14, we can see that both antennas have the capability to provide good service at a short free space distance around 10 meters (60 dB) and different fiber lengths up to 80 m. Figure 4.14 also shows the SNR of the received signal of more than 40 dB when the passive antenna is used and more than 60 dB when active antenna is used with same SMF length of 80 km.

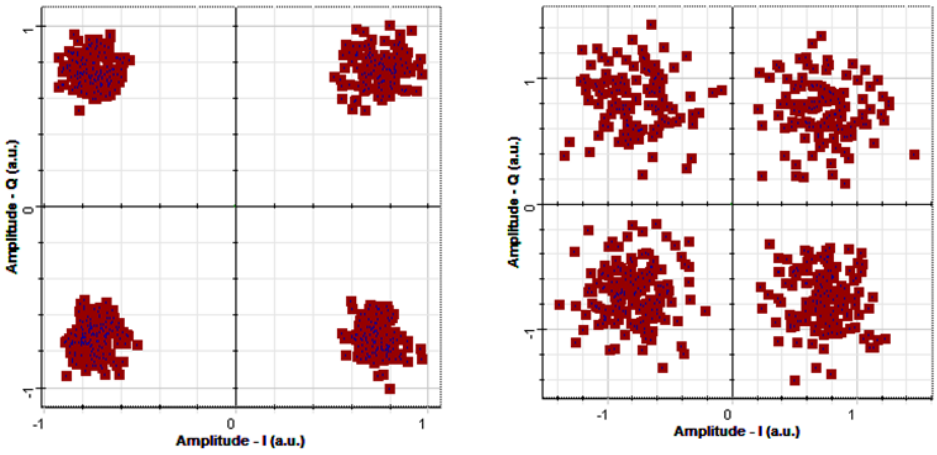

a) b)

Figure 4.15. Constellation diagrams of the received signal from (a) OFDM active antenna at FSL of 70 dB and 60km fiber length with SNR=17.6 dB and (b) OFDM passive at FSL of 60 dB and 60km fiber length with SNR=8.24 dB [38].

The results also contain the constellation diagrams that were obtained from the simulations. Figure 4.15 shows a comparison between the active antenna and the passive antenna for a fiber length of 60 km and different FSL values. For example, figure 4.15a shows clear constellation signals at 70 dB FSL with a received S/N of 17.6 dB from the active patch antenna. Figure 4.15b shows a distorted constellation signal at only 60 dB FSL with a received S/N of 8.24 dB from the passive patch antenna. As a result, we can

conclude from both figures, the passive patch antenna has a limited service under the effects mainly of free space path losses and a longer fiber length.

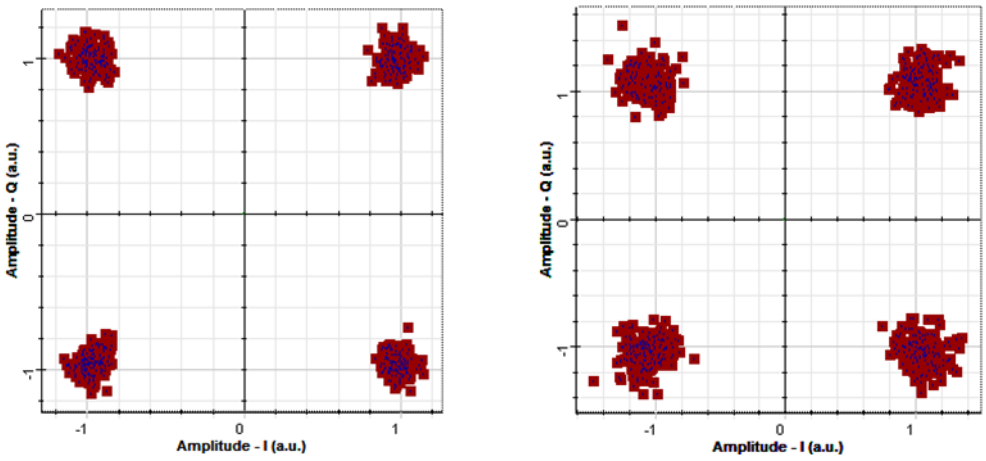

a) b)

Figure 4.16. Constellation diagrams of the received signal from the OFDM active antenna at FSL of 60 dB for (a) 1 km fiber length, BER=0, and S/N=51.29, and (b) 80 km fiber length, BER<$10^{-15}$and S/N=19.54.

Figure 4.16 shows the constellation diagrams for the active antenna performance at FSL of 60 dB for various fiber lengths. Even though there is a huge difference in fiber lengths in figure 4.16a and figure 4.16b, the shape of the constellations is close. This means that the dominant effect on the system comes from the free space path losses. Also, the results can be expressed in term of S/N where 51.29 dB and 19.54 dB S/N are obtained from both scenarios as shown in the caption of figure 4.16. Also, the system performance can be determined by the BER values obtained by simulations. In other words, in the case of short fiber lengths as in figure 4.16a, the signal is received with error-free and BER=0, and in the case of very long fiber lengths, the signal is degraded but the BER is still less than 10^{-15}.

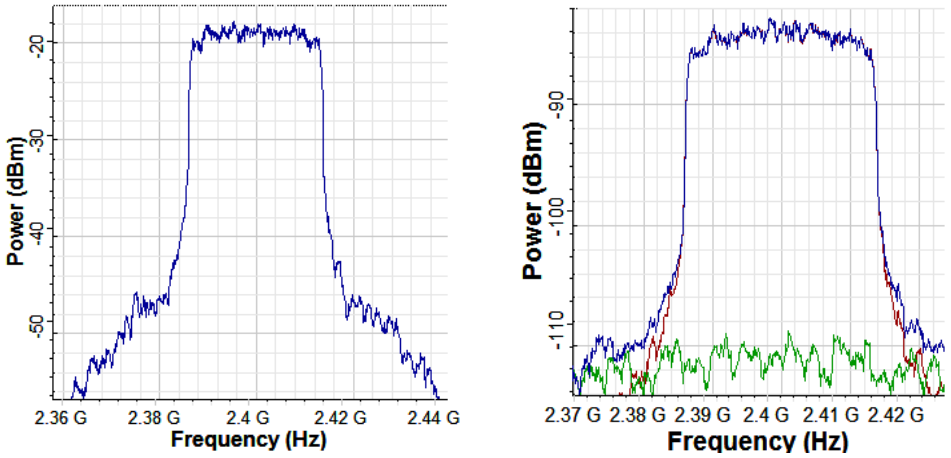

Figure 4.17. a) Transmitted OFDM signal b) Received OFDM signal after 1.2km MMF fiber length and 80 dB path loss [66]

Figure 4.17 depicts the transmitted and received OFDM signal over the designed integrated optical wireless link. The signal is received after traveling 1.2 km through an optical MMF, and it retains its shape even after 30 meter distance in free space propagation. Also, in this section, we demonstrate the obtained results from experiments related to the MMF such as the relationship between EIRP and SNR values for the patch antennas with different fiber lengths and free space distance.

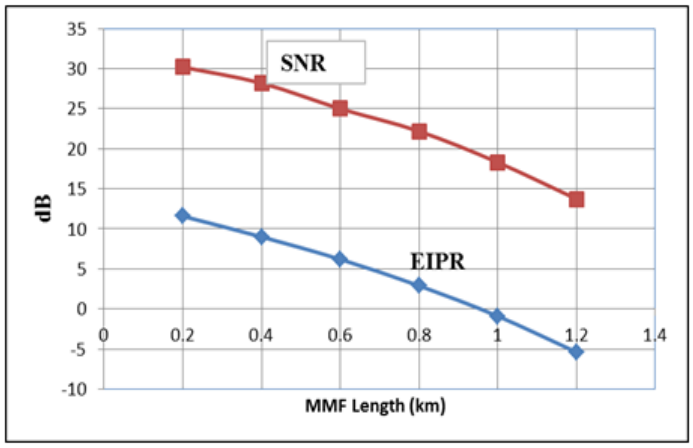

Figure 4.18. MMF length vs EIRP and SNR at an FSL of 70 dB [66]

It is observed from figure 4.18, both EIRP and SNR decrease with an increase of MMF fiber length. Also, figure 4.18 shows the relationship between EIRP and S/N and the MMF length. The BER is observed at 1.2 km fiber length, and of 70 dB free space loss is about 3.1x10-14. After 1.2 km fiber distance, the SNR sharply decreases; however, this is because of the fiber dispersion effects on MMFs.

4.4 Optical OFDM Based W-LAN System with MZM External Modulator

4.4.1 Introduction

In this section, both downlink and uplink optical OFDM scenarios using MZM are presented. In fact, the system setup is the same as in section 4.3 for the downlink; however, the only difference is an external modulator MZM is added to the optical link to enhance the optical power in the system for better performance. For the uplink block diagram, the system is explained in detail. The results are presented for both scenarios.

4.4.2 Downlink system model

In this analog optical link, we adopt the CW laser. This laser generates a CW optical signal. Its average output power is a parameter that you specify. The CW laser phase noise is modeled using the probability density function as in equation (4.9):

$$f(\Delta\emptyset) = \frac{1}{2\pi\sqrt{\Delta f dt}} . e^{-\frac{\Delta\emptyset^2}{4\pi\Delta f dt}} \tag{4.9}$$

where $\Delta\emptyset$ is the phase difference between two successive time instants, and it is the time discretization.

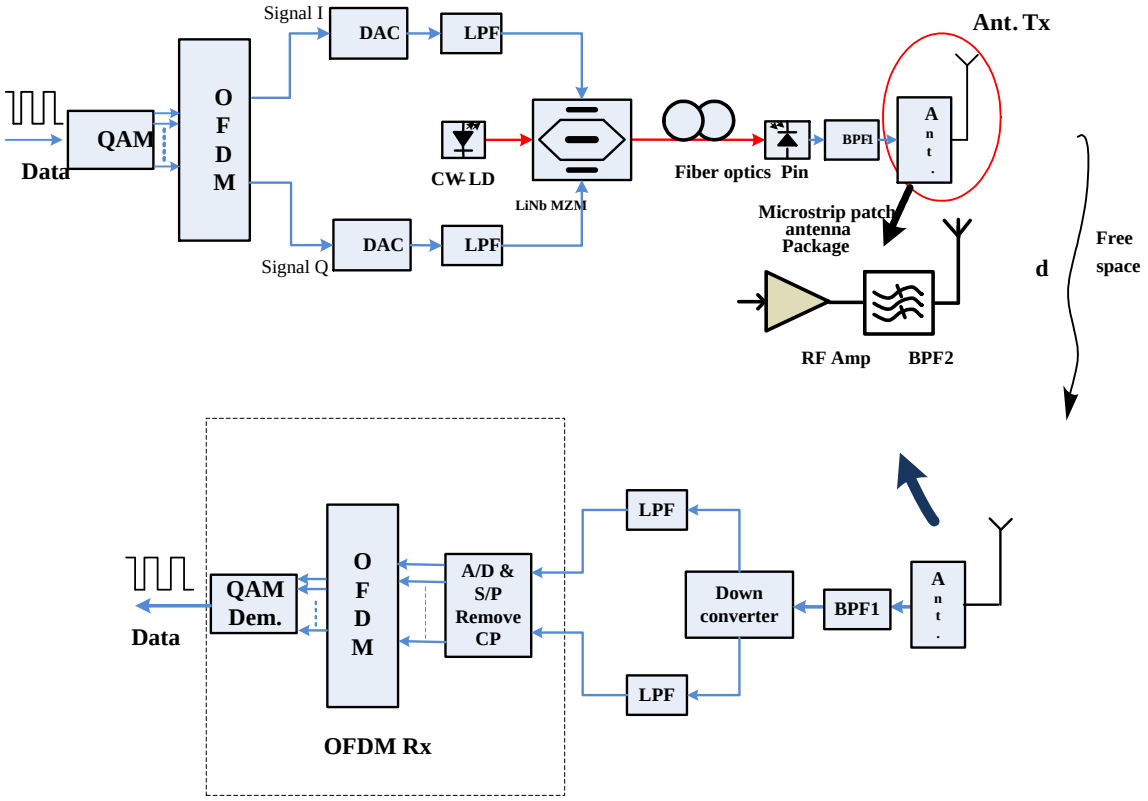

Figure 4.19. Down-link block diagram of an optical OFDM based W-LAN system with a LiNb. MZM external modulator.

- **External modulator**

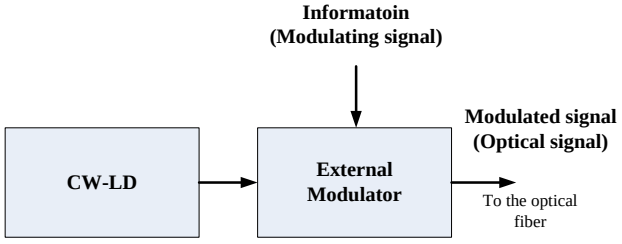

Figure 4.20. External modulator diagram

The optical signal generated by an optical laser source has to be modulated by the information signal before being transmitted over the optical fiber. This can be achieved by directly modulating the bias current of a semiconductor laser or by using an external modulator as in figure 4.19. In the second method, a semiconductor LD is commonly biased at constant current to provide CW output, and external modulators are used to impose the information signal to be transmitted. The most popular external modulators are Mach–Zehnder modulators, and electroabsorption modulators.

- **Mach-Zehnder Modulator (MZM)**

The Mach-Zehnder modulator is an intensity modulator based on an interferometric principle. It consists of two 3 dB couplers which are connected by two waveguides of equal length (see figure 4.21. Because of an electro-optic effect, an externally applied voltage can be used to vary the refractive indices in the waveguide branches.

The different paths can lead to constructive and destructive interference at the output, depending on the applied voltage. Then the output intensity can be modulated according to the voltage.

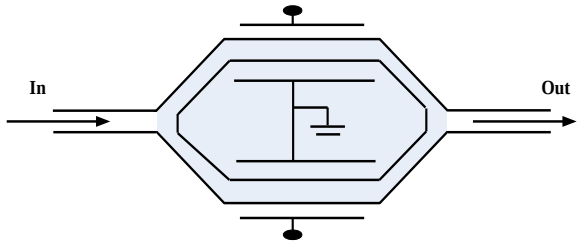

Figure 4.21. A simple sketch diagram of LiNb MZM external modulator

This component simulates a Lithium Niobate MZM based on measured parameters. A DC voltage is required to turn the modulator from the OFF state to the ON

state, or vice versa. Table 4.4 lists the used LiNb MZM properties that were used in these simulations for both downlink and uplink configurations.

Table 4.4 LiNb MZM properties

Parameters	**Value**
Extinction ratio	30 dB
Insertion loss	2dB
Switching bias voltage	4V
Switching RF voltage	4V
Modulation voltage 1	2V
Modulation voltage 2	-2V

4.4.3 Simulation setup

Figure 4.19 shows the typical block diagram of an integrated optical OFDM wireless link with an external modulator. This block diagram consists of an OFDM transmitter and receiver, optical components and the microstrip patch antenna and the modeled FSPL. The same parameters are used as in figure 4.6 and Table 4.3. Each stream of data is assigned to 48 OFDM subcarriers; the total number of subcarriers represents one OFDM symbol. However, 128 OFDM subcarriers are used in this simulation setup as well. The relationship between the frequency spacing Δf and subcarrier frequencies can be defined as $\Delta f = 1/Ts$, where Ts is the OFDM symbol period. Next, the *CP* is appended to each OFDM symbol to reduce the effect of channel dispersion in the fiber link and to mitigate the ICI caused by multipath channels.

4.4.4 Downlink simulation results

Figure 4.22. illustrates the 16-QAM signal constellations received from the OFDM transmitter over a 50 km SMF and after propagation through a 70 dB free-space link. The BER=0 and the signal preserved its shape through all ways.

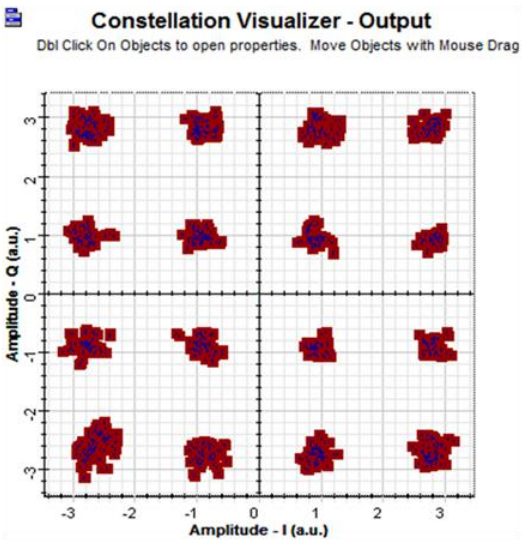

Figure 4.22. Constellation diagram of OFDM received signal: 50 km SMF fiber length and 70 dB

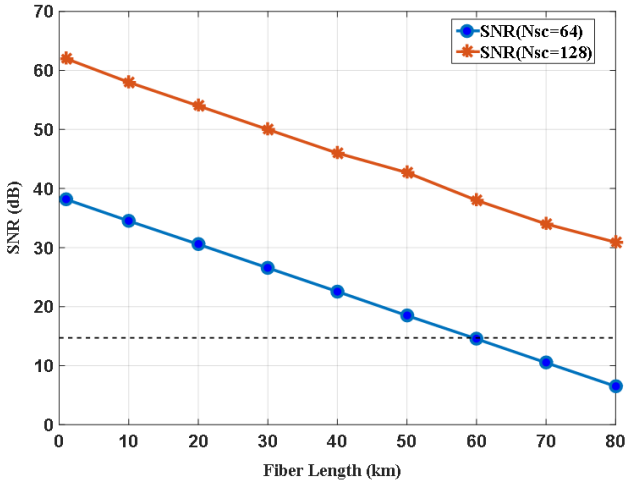

Figure 4.23. Fiber length vs. SNR for OFDM *Nsc*=64 and *Nsc*=128.

The downlink configuration for the optical OFDM system with the external modulator is presented. In fact, two sets of OFDM subcarriers were tested using the simulations. The results are illustrated in figure 4.23. Figure 4.23 shows the relationship between the fiber length in km and the SNR in dB. The blue curve presents the SNR against the fiber length for N_{SC}= *64* subcarriers set, while the orange curve presents the SNR against the fiber length for N_{SC}=*128* subcarriers set. From the figure, it can be seen that the SNR in the case of the 128 subcarriers set is higher than the SNR of the 64 subcarriers with more than 24 dB. Also, it is observed that as the distance increases, the performance is degraded due to dispersion.

The relationship between the SNR and BER for N_{SC}=*64* subcarriers is depicted in figure 4.24. It can be seen that at a lower SNR, the BER is high and the BER decreases, whereas the SNR increases. Meanwhile, the OSNR at 25 dB is achieved.

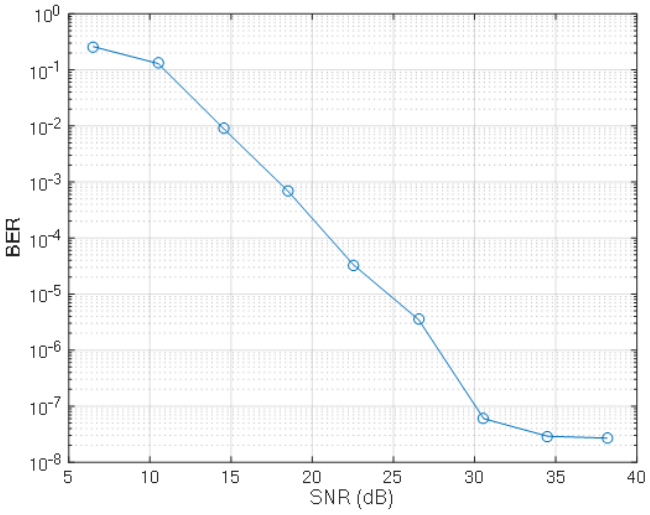

Figure 4.24. SNR vs. BER for OFDM *Nsc*=64.

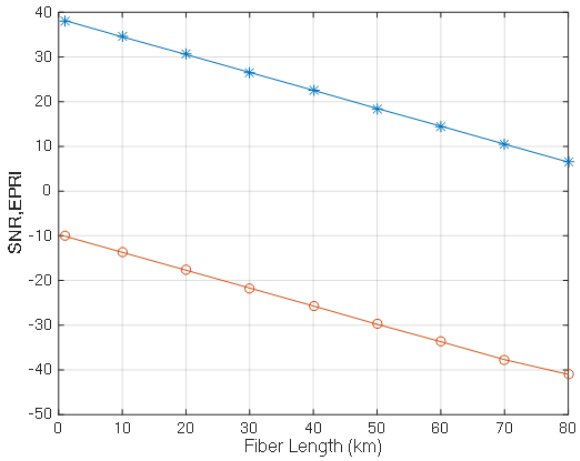

Figure 4.25. Fiber length vs. SNR and EIRP for N_{SC}=64

Figure 4.25 shows the effect of the fiber length on the EIRP and then on the SNR for N_{SC}=64. SNR decreases linearly with the decrease of the EIRP. The signal is degraded severely at a fiber length of 80 km because of the effect of the chromatic dispersion on SMFs.

4.4.5 Uplink system model

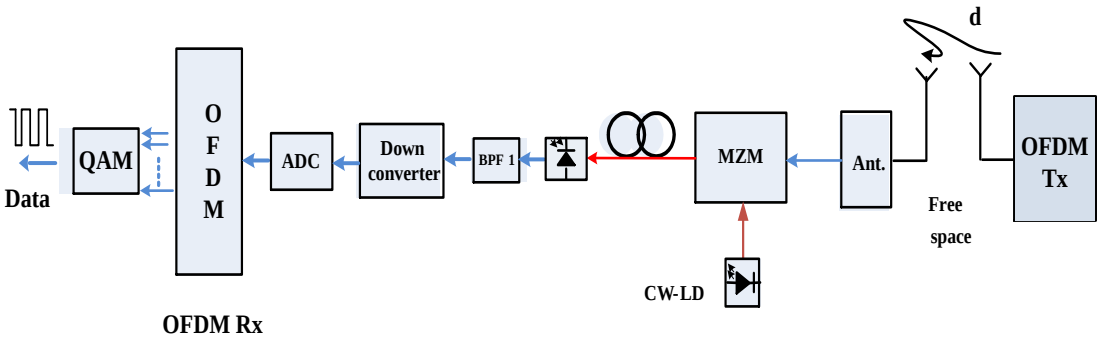

Figure 4.26. Uplink block diagram of an optical OFDM based W-LAN system with a LiNb. MZM external modulator.

Figure 4.26. illustrates the block diagram for the proposed optical OFDM-based W-LAN for uplink. The same parameters of the downlink are used, and a CW laser source is adopted.

4.4.6 Uplink simulation results

The purpose of this simulation is to investigate the microstrip antenna under this condition where the signal is sent from the user through the antenna over the fiber. The signal is transmitted through 80 dB in free space and then carried over a 40 km SMF. The signal still preserves its strength.

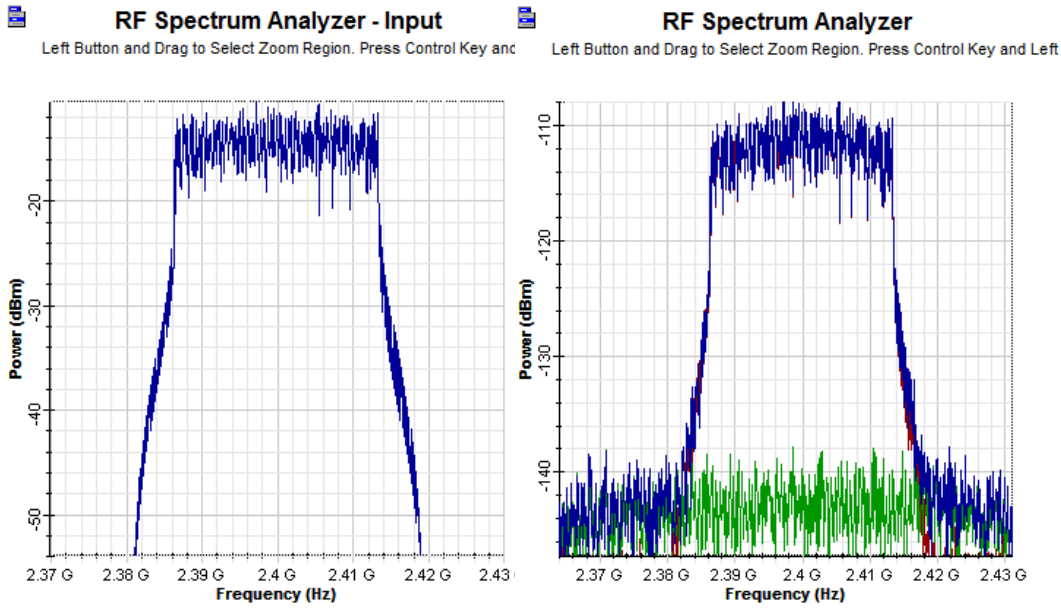

a) b)

Figure 4.27. a) Transmitted OFDM signal for uplink scenario b) Received OFDM signal after 40 km SMF fiber length, OSNR=38 dB and 80 dB path loss and SNR=28.8 dB

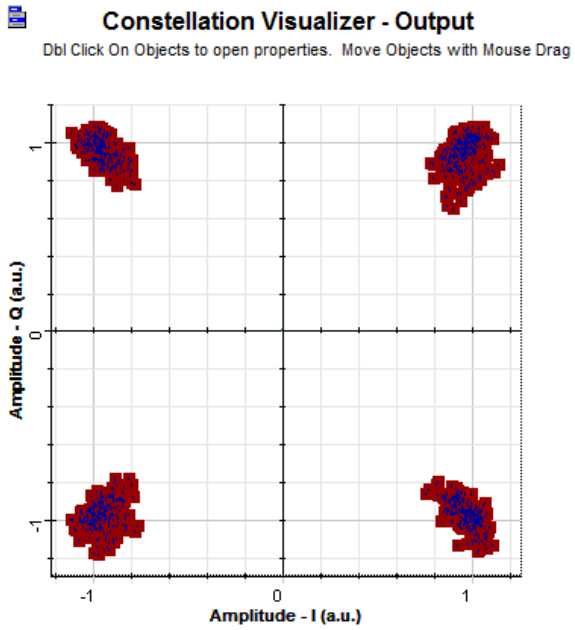

Figure 4.28. Uplink received OFDM constellation 40 km SMF fiber long, OSNR=38 dB and 80 dB path loss AT SNR=28.8 dB

Another measure used to test the transmitted signal is the signal constellation visualizer. From figure 4.28, it can be seen that the signal is reconstructed using a 4-QAM modulator at the receiver end. The shape of the constellations supports the information obtained from the received spectrum. Even the signal launched with a very low signal power at the external modulator around -2 dB for uplink scenario, but the results show that the system performance is very efficient to support this service to the destination.

Chapter Five: Conclusions and Future Work

5.1 Conclusions

This study shows the application of OFDM is suitable for the combination of wireless and optical communications for last mile purposes. The proposed optical OFDM system has been designed and implemented using Optisystem optical communication software tools. Many models and simulations have been used to facilitate understanding of the behavior of the proposed modeling blocks. There was a clear incompatibility between OFDM modulation and conventional optical systems. Recently, some forms of OFDM that may overcome these incompatibilities in different ways have been developed for a variety of optical applications.

This research has presented some detailed scenarios related to OFDM applications, including the analysis and design of a microstrip patch antenna. The obtained s-parameters were implemented in both conventional optical and proposed optical OFDM block diagrams. The demonstration of the implementation scenario of the microstrip patch antenna in the proposed optical modeling systems has shown that the passive microstrip patch antenna can cover a short distance of 10 meters. However, an active microstrip patch antenna would work better if a large coverage area is desired. Meanwhile, the results' measurements and discussion took place in this research in terms of EIRP, signal noise, OSNR, S/N, and BER at different points of the signal process in the systems. The results showed that the passive microstrip patch antenna has a limited

capability compared to the active microstrip patch antenna regarding the radiation distance at the same operating frequency.

The proposed optical OFDM based W-LAN systems that can carry OFDM signals with a 2.4 GHz radio frequency over a cost-effective optical link are cost-effective because the signal is processed locally at the CO, and no active optical components, such as optical amplifiers, are used in the system.

The required microstrip patch antenna parameters of the proposed systems have been analyzed and designed. The microstrip patch antenna (S-parameters) were loaded into the Optisystem communication software tool in *Touchstone format*. As a result, this achievement gives a great impetus to design an integrated optical-wireless system and simulation results validate the proposed technique.

The DML was used for conventional optical and optical OFDM links, while the CW laser source was employed in optical OFDM down-link and up-link blocks when an MZM external modulator was utilized. In addition, the LiNb. MZM external modulator was utilized to enhance the system launched power when higher level M-QAM such as 16-QAM was used. In conventional optical systems, both passive and active antennas were implemented. The results show that the passive microstrip patch antenna has a limited service distance of 10 meters. On the other hand, the active microstrip patch antenna can increase the coverage up to 50 meters in free space distance when an SMF is used.

In optical OFDM-based W-LAN systems, a comparison took place between the systems' configurations that adopted active and passive antennas. The results indicate

that the integration of an optical OFDM with an active microstrip antenna can enhance system reliability in terms of the service coverage area. The required minimum OSNR was obtained in achieving a BER of 1.0 10^{-3} over the optical dispersive channel. Moreover, this integration provides higher SNR and better performance for the last mile.

In this study, an optical OFDM based W-LAN with an external modulator was designed and simulated. The external modulator MZM was used in the down-link block diagram to increase optical power when the 16-QAM modulator is used. By using this model, the results were obtained and analyzed in terms of OSNR EIRP, SNR, signal constellations and BER. The results showed that this integrated optical wireless link is very robust for carrying OFDM-based wireless LAN signals over an optical fiber. Also, the optical OFDM uplink system with external modulator was modeled and simulated. The results were illustrated and showed that this model helps to increase the coverage service to more than 30 meters when an SMF of 80 km length is utilized.

The MMF was used in this dissertation as well. This fiber was utilized to connect the system with the proposed active antenna. The system was simulated as shown in chapter 4. The results were illustrated, and the BER was obtained with a value of ($3.1x10^{-14}$) at 1.2 km fiber length, and of 70 dB free space loss. After 1.2 km fiber distance, the SNR sharply decreases; however, this is because of the fiber dispersion effects on MMFs.

In conclusion, the integration of optical OFDM based-W-LAN and an active microstrip patch antenna can provide sufficient service for the last mile up to 80 km on SMF and more than 50 meters wirelessly.

5.2 Future Work

- There is still a gap in how MMF can be utilized to achieve better results. In this research, the focus was on two types of laser sources: DML and CW. Alternatively, another laser source could be a better solution that leads to a better performance along side with MMF. The vertical cavity surface emitting laser (VCSEL) is a very strong candidate to be used as an alternative laser source for MMF links. This is because of its cost-effective and other common advantages.
- The considered environment in this work's simulations was a LOS, where the signal is traveling in a straight line from the wireless antenna to the end user. Another scenario could be considered as a future work, where multipath-fading is present in wireless networks. This provides us with a comprehensive understanding of how the system performs.
- Integrating WDM with an array of microstrip patch antennas would be practical in certain applications. Therefore, this scenario can be applied for both wireless LAN and WiMax network as well as 5G networks.

References

[1] Weinstein, S. B. (2009). The history of orthogonal frequency-division multiplexing [History of Communications]. *IEEE Communications Magazine*, *47*(11).

[2] Yao, P. (2009, December). Advanced OFDM system for modern communication networks. In Proceedings of the Second Symposium International Computer Science and Computational Technology (ISCSCT'09) (pp. 475-478).

[3] Cho, Y. S., Kim, J., Yang, W. Y., & Kang, C. G. (2010). *MIMO-OFDM wireless communications with MATLAB*. John Wiley & Sons.

[4] Hwang, T., Yang, C., Wu, G., Li, S., & Li, G. Y. (2009). OFDM and its wireless applications: A survey. *IEEE Transactions on Vehicular Technology*, *58*(4), 1673-1694.

[5] LaSorte, N., Barnes, W. J., & Refai, H. H. (2008). The history of orthogonal frequency division multiplexing. In *Global Telecommunications Conference, 2008. IEEE GLOBECOM 2008. IEEE* (pp. 1-5). IEEE.

[6] Armstrong, J. (1999). Analysis of new and existing methods of reducing intercarrier interference due to carrier frequency offset in OFDM. *IEEE transactions on communications*, 47(3), 365-369.

[7] Armstrong, J. (2009). OFDM for optical communications. Journal of lightwave technology, 27(3), 189-204.

[8] Giddings, R. (2014). Real-time digital signal processing for optical OFDM-based future optical access networks. Journal of Lightwave Technology, 32(4), 553-570.

[9] Cooley, J. W., & Tukey, J. W. (1965). An algorithm for the machine calculation of complex Fourier series. *Mathematics of computation*, *19*(90), 297-301.

[10] Chang, R.W. (1966). Synthesis of band-limited orthogonal signals for multichannel data transmission. Bell Systems Tech. Journal, vol. 45, pp.1775–1796.

[11] Chang, R.W. (1970). Orthogonal frequency division multiplexing. U.S. Patent No. 3, 488, 4555, filed November 14, 1966, issued Jan.1970.

[12] Weinstein, S., & Ebert, P. (1971). Data transmission by frequency-division multiplexing using the discrete Fourier transform. *IEEE Transactions on Communication Technology*, *19*(5), 628-634.

[13] Peled, A., & Ruiz, A. (1980, April). Frequency domain data transmission using reduced computational complexity algorithms. In *Acoustics, Speech, and Signal*

Processing, IEEE International Conference on ICASSP'80. (Vol. 5, pp. 964-967). IEEE.

[14] Yang, Q., Amin, A. Al, & Shieh, W. (2011). *Impact of Nonlinearities on Fiber Optic Communications*. Chapter 2, optical OFDM basics.

[15] Mandke, K., Nam, H., Yerramneni, L., & Zuniga, C. (2003). The evolution of UWB and IEEE 802.15. 3a for very high data rate WPAN. *EE 381K-11 Wireless Communications UWB Group, The University of Texas at Austin*.

[16]Koffman, I., & Roman, V. (2002). Broadband wireless access solutions based on OFDM access in IEEE 802.16. IEEE communications magazine, 40(4), 96-103.

[17]Ismail, T., Chuang, C. H., & Seeds, A. J. (2008). Wireless data transmission of IEEE802.11a signals over fibre using low cost uncooled directly modulated lasers. *2008 IEEE International Meeting on Microwave Photonics Jointly Held with the 2008 Asia-Pacific Microwave Photonics Conference, MWP2008/APMP2008*, 70–73.

[18] Cox, C. H. (2006). *Analog optical links: theory and practice*. Cambridge University Press.

[19] Das, A., Mjeku, M., Nkansah, A., & Gomes, N. J. (2007). Effects on IEEE 802.11 MAC throughput in wireless LAN over fiber systems. Journal of Lightwave Technology, 25(11), 3321-3328.

[20] Crisp, M. J., Li, S., Watts, A., Penty, R. V., & White, I. H. (2007). Uplink and downlink coverage improvements of 802.11 g signals using a distributed antenna network. Journal of Lightwave Technology, 25(11), 3388-3395.

[21] Molisch, A. F. (2009). Ultra-Wide-Band Propagation Channels. *Proceedings of the IEEE*, *97*(2), 353–371.

[22] Llorente, R., Alves, T., Morant, M., Beltran, M., Perez, J., Cartaxo, A., & Marti, J. (2008). Optical Distribution of OFDM and Impulse-Radio UWB in FTTH networks. *Communications*, 8–10.

[23] Kenshil, S., Rashwan, G., & Matin, M. (2012). Multiband OFDM-UWB signals over hybrid fiber-wireless Link (Vol. 8498, p. 849803).

[24] Ran, M. (2008). Selection of UWB technology for UWB Radio over Fiber. *History*, 1–51.

[25] Guennec, Y. Le, Pizzinat, A., Meyer, S., Charbonnier, B., Lombard, P., Lourdiane, M., … Sillans, C. (2009). Low-Cost Transparent Radio-Over-Fiber System for In-Building Distribution of UWB Signals. *Lightwave*, *27*(14), 2649–2657.

[26] Ran, M., Lembrikov, B. I., & Ben Ezra, Y. (2010). Ultra-Wideband Radio-Over-Optical Fiber Concepts, Technologies and Applications. *IEEE Photonics Journal*, *2*(1), 36–48.

[28] Kshetrimayum, S. (2009). An introduction to UWB communication systems. *Ieee Potentials*, (April), 9–13.

[29] Batra, A., Balakrishnan, J., Aiello, G. R., Foerster, J. R., & Dabak, A. (2004). Design of a Multiband OFDM System for Realistic UWB Channel Environments, *52*(9), 2123–2138.

[30] Molisch, A. F., Foerster, J. R., & Pendergrass, M. (2003). Channel models for ultra-wide-band personal area networks. *IEEE Wireless Communications*, *10*(6), 14–21.

[31] Cassioli, D., Member, S., Win, M. Z., Member, S., & Molisch, A. F. (2002). The Ultra-Wide Bandwidth Indoor Channel : From Statistical Model to Simulations, *20*(6), 1247–1257.

[32] Ran, M., Lembrikov, B. I., & Ben Ezra, Y. (2010). Ultra-Wideband Radio-Over-Optical Fiber Concepts, Technologies and Applications. *IEEE Photonics Journal*, *2*(1), 36–48.

[33] St, G., Holon, P. O. B., & Url, S. (2008). Ultra-Wideband Radio-over-optical Fiber : technologies and applications, *3*, 149–151.

[34] Nee, R. V., & Prasad, R. (2000). OFDM for wireless multimedia communications. Artech House, Inc., Boston, USA.

[35] Djordjevic, I. B., & Vasic, B. (2006). Orthogonal frequency division multiplexing for high-speed optical transmission. *Optics Express*, *14*(9), 3767-3775.

[36] Rashwan, G., Kenshil, S., & Matin, M. (2012, October). PAPR reduction in OFDM WiMAX application. In *Optics and Photonics for Information Processing VI* (Vol. 8498, p. 849805). International Society for Optics and Photonics.

[37] Rashwan, G., Kenshil, S., & Matin, M. (2013, September). PAPR mitigation algorithms for OFDM WiMAX link. In *Optics and Photonics for Information Processing VII* (Vol. 8855, p. 88550D). International Society for Optics and Photonics.

[38] Kenshil, S., Rashwan, G., & Matin, M. (2013, September). Implementation of a photonic antenna in optical OFDM link. In *Optics and Photonics for Information Processing VII* (Vol. 8855, p. 88550B). International Society for Optics and Photonics.

[39] Dhivagar, B., Madhan, M. G., & Fernando, X. (2007, August). Analysis of OFDM signal through optical fiber for Radio-over-Fiber transmission. In *Access Networks & Workshops, 2007. AccessNets' 07. Second International Conference on* (pp. 1-8). IEEE.

[40] Djordjevic, I. B., & Vasic, B. (2006). Orthogonal frequency division multiplexing for high-speed optical transmission. *Optics Express*, *14*(9), 3767-3775.

[41] Agrawal, GP. (2002). Fiber-optic communication systems, 3rd edn.Wiley, New York .

[42] Agrawal, GP. (2004). Lightwave technology: components and devices.Wiley, New York.

[43] Agrawal, GP. (2005). Lightwave technology: telecommunication systems. Wiley, New York.

[44] Keiser, G. (2003). *Optical fiber communications*. John Wiley & Sons, Inc.

[45] Ghassemlooy, Z., Popoola, W., & Rajbhandari, S. (2012). *Optical wireless communications: system and channel modelling with Matlab®*. CRC press.

[46] Djordjevic, I., Ryan, W., & Vasic, B. (2010). *Coding for optical channels*. Chapter 2.

[47] http://www.fiberopticsonline.com/doc/understanding-and-measuring-chromatic-dispers-0002.

[48] Power budget and loss budget available at: http://www.thefoa.org/tech/lossbudg.htm: Accessed April 2017.

[49] Al-Raweshidy, H., & Komaki, S. (2002). Radio over fiber technologies for mobile communications networks. Artech House.

[50] Qian, D., Cvijetic, N., Hu, J., & Wang, T. (2009, March). Optical OFDM transmission in metro/access networks. In Optical Fiber Communication Conference (p. OMV1). Optical Society of America.

[51] Shieh, W., & Athaudage, C. (2006). Coherent optical orthogonal frequency division multiplexing. *Electronics letters*, *42*(10), 587-589.

[52] Schmidt, B. J., Lowery, A. J., & Armstrong, J. (2008). Experimental demonstrations of electronic dispersion compensation for long-haul transmission using direct-detection optical OFDM. Journal of Lightwave Technology, 26(1), 196-203.

[53] Margariti, K., & Kamalakis, T. (2014, October). Coherent Optical Wireless Systems for High Speed Local Area Networks with Increased Resilience. In *Proceedings of the 18th Panhellenic Conference on Informatics* (pp. 1-5). ACM.

[54] Yi, X., Shieh, W., & Tang, Y. (2007). Phase estimation for coherent optical OFDM. *IEEE Photonics Technology Letters*, *19*(12), 919-921.

[55] Shieh, W., Chen, W., & Tucker, R. S. (2006). Polarisation mode dispersion mitigation in coherent optical orthogonal frequency division multiplexed systems. *Electronics Letters*, *42*(17), 1.

[56] Shieh, W., Bao, H., & Tang, Y. (2008). Coherent optical OFDM: theory and design. Optics express, 16(2), 841-859.

[57] Cvijetic, M. (2004) Optical transmission systems engineering. Artech House, Boston, MA 2.

[58] Schimpf, A., Bucci, D., & Cabon, B. (2009). Optimum biasing of VCSEL diodes for all-optical up-conversion of OFDM signals. *Journal of Lightwave Technology*, *27*(16), 3484-3489.

[59] Ramaswami, R. Sivarajan, K. (2002) Optical networks: a practical perspective, 2nd edn. Morgan Kaufman, San Fransisco, CA.

[60] James, J. R., & Hall, P.S. (Eds.). (1989). Handbook of microstrip antennas. (Vol. 28), IET.

[61] CST-Computer Simulation Technology. Antenna design and simulation. [online]. Available At: https://www.cst.com/Applications/Category/Antenna+Design+and+Simul-ation.

[62] Deschamps, G. A. (1953). Microstrip microwave antennas. In Proceedings of the Third Symposium on the USAF Antenna Research and Development Program, Oct (pp. 18-22).

[63] Gutton, H., & Baissinot, G. (1955). Flat aerial for ultra high frequencies. French patent, 703113.

[64] Pozar, D. M. (1992). Microstrip antennas. Proceedings of the IEEE, 80(1), 79-91.

[65] Balanis, C.A., (2005). Antenna Theory: Analysis design. Third Edition, John Wiley & Sons, Inc, chapter 14, pp811-869.

[66] Kenshil, S., Rashwan, G., & Matin, M. (2017, January). Analysis of optical OFDM based wireless LAN. In Computing and Communication Workshop and Conference (CCWC), 2017 IEEE 7th Annual (pp. 1-5). IEEE.

[67] Mutiara, A. B., & Refianti, R. (2011). Rachmansyah "Design of micro strip antenna for wireless Communication at 2.4 GHz"* Journal of Theoretical and Applied Information Technology Vol. 33 Gunadarma university.

[68] Nakar, P. S. (2004). Design of a compact microstrip patch antenna for use in wireless/cellular devices.

[69] Balanis, C.A., (1997). Antenna theory: Analysis and design. John Wiley & Sons, Inc.

[70] Gupta, K. C., & Hall, P. S. (Eds.). (2000). Analysis and design of integrated circuit-antenna modules. Wiley.

[71] Kenshil, S., Rashwan, G., & Matin, M. (2013). Implementation of a photonic antenna in optical OFDM link. In Optics and Photonics for Information Processing VII (Vol. 8855, p. 88550B). International Society for Optics and Photonics.

[72] Kenshil S., Rashwan G., Matin M. (2018, March). Investigation and Analysis of Using Microstrip Patch Antenna in Optical OFDM Systems. *IPASJ International Journal of Electronics & Communication (IIJEC).*

[73] Pozar, D. (2005). Microwave engineering. John Wiley and Sons, 3rd, USA.

[74] Sittakul, V. and Cryan, M. J. (2007). A 2.4-GHz wireless-over-fiber system using photonic active integrated antennas (PhAIAs) in ad hoc and infrastructure ode in Microwave Conference, APMC 2007. Asia-Pacific.

[75] Prakoso, T., Ngah, R., Ghassemlooy, Z., & Rahman, T. A. (2011). Antenna representation in two-port network scattering parameter. *Microwave and Optical Technology Letters*, *53*(6), 1404-1409.

[76] Sobhy, M. I., Sanz-Izquierdo, B., & Batchelor, J. C. (2007). System and circuit models for microwave antennas. *IEEE Transactions on Microwave Theory and Techniques*, *55*(4), 729-735.

[77] Nakar, P. S. (2004). Design of a compact Microstrip Patch Antenna for use in Wireless / Cellular Devices. *Diginole.Lib.Fsu.Edu/Cgi*. Retrieved from http://diginole.lib.fsu.edu/cgi/viewcontent.cgi?article=3420&context=etd

[78] OptiSystem, (2014). Low Pass Cosine Roll off Filter. Tutorials Volume 1, Optical Communication System Design Software.

[79] Erceg, V., Greenstein, L. J., Tjandra, S. Y., Parkoff, S. R., Gupta, A., Kulic, B., & Bianchi, R. (1999). An empirically based path loss model for wireless channels in

suburban environments. IEEE Journal on selected areas in communications, 17(7), 1205-1211.

[80] Friis, H. T. (1946). A note on a simple transmission formula. Proceedings of the IRE, 34(5), 254-256.

[81] Power Budget and Loss Budget available at: http://www.thefoa.org/tech/lossbudg.html: Accessed April 2017.

[82] Sauer, M., Kobyakov, A., Hurley, J. E., & George, J. (2005, October). Experimental study of radio frequency transmission over standard and high-bandwidth multimode optical fibers. In Microwave Photonics, 2005. MWP 2005. International Topical Meeting on (pp. 99-102).

[83] Fernando, X. (2006, September). Radio over fiber in multimedia access networks. In Proceedings of the 1st international conference on Access networks (p. 3). ACM.

[84] Lowery, A. J., & Armstrong, J. (2006). Orthogonal-frequency-division multiplexing for dispersion compensation of long-haul optical systems. Optics Express, 14(6), 2079-2084.

[85] Cseh, T., & Udvary, E. (2011, July). Cost effective RoF with VCSELs and multimode fiber. In Networks and Optical Communications (NOC), 2011 16th European Conference on (pp. 60-63).

[86] Larsson, A., Carlsson, C., Gustavsson, J., Haglund, A., & Modh, P. (2004, October). Broadband direct modulation of VCSELs and applications in fiber optic RF links. In Microwave Photonics, 2004. MWP'04. 2004 IEEE International Topical Meeting on (pp. 251-254).

[87] Gomes, N. J., Nkansah, A., & Wake, D. (2008). Radio-over-MMF techniques—Part I: RF to microwave frequency systems. Journal of lightwave technology, 26(15), 2388-2395.

[89] Cvijetic, N., Qian, D., & Hu, J. (2010). 100 Gb/s optical access based on optical orthogonal frequency-division multiplexing. IEEE Communications Magazine, 48(7).

[90] Herlekar, S. R., Matarneh, K. Z., Wu, H. C., Wu, Y., & Wang, X. (2005). Performance evaluation of an ICI self-cancellation coded transceiver for mobile DVB-T applications. IEEE Transactions on Consumer Electronics, 51(4), 1110-1120.

[91] Litwin, L., & Pugel, M. (2001). The principles of OFDM. RF signal processing, 2, 30-48.

[92] Weinstein, S. B. (2009). Introduction to the History of OFDM. IEEE Communications Magazine, 47(11).

[93] Armstrong, J. (2008, October). OFDM for next generation optical communication systems. In Optical Internet, 2008. COIN 2008. 7th International Conference on (pp. 1-2). IEEE.

[94] Gomes, N. J., Morant, M., Alphones, A., Cabon, B., Mitchell, J. E., Lethien, C., ... & Iezekiel, S. (2009). Radio-over-fiber transport for the support of wireless broadband services. Journal of Optical Networking, 8(2), 156-178.

[95] Qian, X., Hartmann, P., Ingham, J. D., Diab, A., Penty, R. V., & White, I. H. (2004, October). Modelling and simulation-based prediction of radio transmission over multimode fibre. In Microwave Photonics, 2004. MWP'04. 2004 IEEE International Topical Meeting on (pp. 165-168).

[96] Sakran, H., Shokair, M., & Elazm, A. A. (2008, October). An efficient technique for reducing PAPR of OFDM system in the presence of nonlinear high power amplifier. In Signal Processing, 2008. ICSP 2008. 9th International Conference on (pp. 1749-1752).

[97]Benedetto, S., Biglieri, E., & Castellani, V. (1987). Digital Transmission Theory Prentice-Hall. Inc., New Jersey.

List of Publications

[1] Kenshil S., Rashwan G., Matin M. (2018, March). Investigation and Analysis of Using Microstrip Patch Antenna in Optical OFDM Systems. *IPASJ International Journal of Electronics & Communication* (IIJEC). Volume 6, Issue 3.

[2] Rashwan G., Kenshil S., Matin M. (2018, March). The Study of PAPR Reduction Technique Based on Hybrid of PTS and SLM. *IPASJ International Journal of Information Technology* (IIJIT),Volume 6, Issue 3.

[3] Kenshil, S., Rashwan, G., & Matin, M. (2017, January). Analysis of optical OFDM based wireless LAN. In *Computing and Communication Workshop and Conference (CCWC), 2017 IEEE 7th Annual* (pp. 1-5).

[4] Rashwan, G., Kenshil, S., & Matin, M. (2017, January). Analysis of PAPR hybrid reduction technique based on PTS and SLM. In *Computing and Communication Workshop and Conference (CCWC), 2017 IEEE 7th Annual* (pp. 1-4)..

[5] Kenshil, S., Rashwan, G., & Matin, M. (2013, September). Implementation of a photonic antenna in optical OFDM link. In *Optics and Photonics for Information Processing VII* (Vol. 8855, p. 88550B). International Society for Optics and Photonics.

[6] Rashwan, G., Kenshil, S., & Matin, M. (2013, September). PAPR mitigation algorithms for OFDM WiMAX link. In *Optics and Photonics for Information Processing VII* (Vol. 8855, p. 88550D). International Society for Optics and Photonics.

[7] Kenshil, S., Rashwan, G., & Matin, M. (2012, October). Multiband OFDM-UWB signals over hybrid fiber-wireless Link. In *Optics and Photonics for Information Processing VI* (Vol. 8498, p. 849803). International Society for Optics and Photonics.

[8] Rashwan, G., Kenshil, S., & Matin, M. (2012, October). PAPR reduction in OFMD WiMAX application. In *Optics and Photonics for Information Processing VI* (Vol. 8498, p. 849805). International Society for Optics and Photonics.

Appendix A

A.1 File Name: Transmitting.s2p., Touchstone format file.

! Design environment at room temp. Sat Dec 22 14:12:34 pm 2012
!
!freq-unit parameter-type data-format keyword impedance-ohms

!! (GHz) S MA R=50 (Ω)

!Freq	**MagS11**	**AngS11**	**MagS21**	**AngS21**	**MagS12**	**AngS12**	**MagS22**	**AngS22**
2.31	0.6914	45.146	1.0335	0	0	0	0	0
2.32	0.6516	41.61	1.0879	0	0	0	0	0
2.33	0.6046	37.767	1.1434	0	0	0	0	0
2.34	0.5502	33.588	1.1998	0	0	0	0	0
2.35	0.4872	29.094	1.2557	0	0	0	0	0
2.36	0.4144	24.345	1.3092	0	0	0	0	0
2.37	0.3326	19.498	1.3578	0	0	0	0	0
2.38	0.2422	14.983	1.3979	0	0	0	0	0
2.39	0.144	12.350	1.4265	0	0	0	0	0
2.4	0.0465	26.230	1.4412	0	0	0	0	0
2.41	0.0673	150.44	1.4405	0	0	0	0	0
2.42	0.1668	155.94	1.4246	0	0	0	0	0
2.43	0.2621	152.58	1.3951	0	0	0	0	0
2.44	0.3518	147.9	1.3544	0	0	0	0	0
2.45	0.4314	143.01	1.2961	0	0	0	0	0
2.46	0.5019	138.27	1.2436	0	0	0	0	0
2.47	0.5629	133.81	1.1893	0	0	0	0	0
2.48	0.6157	129.67	1.1353	0	0	0	0	0
2.49	0.6608	125.83	1.0823	0	0	0	0	0
2.5	0.699	122.31	1.0321	0	0	0	0	0
2.51	0.7315	119.09	0.9849	0	0	0	0	0
2.52	0.7593	116.14	0.9412	0	0	0	0	0
2.53	0.7829	113.42	0.9004	0	0	0	0	0
2.54	0.8031	110.89	0.8631	0	0	0	0	0
2.55	0.8204	108.58	0.8289	0	0	0	0	0
2.56	0.8354	106.42	0.7977	0	0	0	0	0
2.57	0.8483	104.42	0.7691	0	0	0	0	0
2.58	0.8595	102.51	0.7431	0	0	0	0	0

A.2 File Name: Receiving.s2p.,Touchstone format file.

! Environment room temp. Sat Dec 22 14:12:34 pm 2012
!
!freq-unit parameter-type data-format keyword impedance-ohms

!! (GHz) S MA R=50

!Freq	MagS11	AngS11	MagS21	AngS21	MagS12	AngS12	MagS22	AngS22
2.31	0	0	1.0355	0	0	0	0.6916	45.157
2.32	0	0	1.0883	0	0	0	0.6516	41.621
2.33	0	0	1.1434	0	0	0	0.6048	37.767
2.34	0	0	1.1997	0	0	0	0.5502	33.588
2.35	0	0	1.2557	0	0	0	0.487	29.094
2.36	0	0	1.3094	0	0	0	0.4145	24.345
2.37	0	0	1.3578	0	0	0	0.3326	19.499
2.38	0	0	1.3979	0	0	0	0.2422	14.984
2.39	0	0	1.4266	0	0	0	0.145	12.36
2.4	0	0	1.4413	0	0	0	0.0466	26.231
2.41	0	0	1.4406	0	0	0	0.0674	150.45
2.42	0	0	1.4247	0	0	0	0.1669	155.95
2.43	0	0	1.3951	0	0	0	0.263	152.59
2.44	0	0	1.3545	0	0	0	0.3518	147.9
2.45	0	0	1.296	0	0	0	0.4317	143.02
2.46	0	0	1.2436	0	0	0	0.5021	138.27
2.47	0	0	1.1893	0	0	0	0.5633	133.81
2.48	0	0	1.135	0	0	0	0.6159	129.66
2.49	0	0	1.0823	0	0	0	0.6608	125.83
2.5	0	0	1.0321	0	0	0	0.699	122.32
2.51	0	0	0.9849	0	0	0	0.7316	119.1
2.52	0	0	0.941	0	0	0	0.7593	116.14
2.53	0	0	0.9004	0	0	0	0.7829	113.42
2.54	0	0	0.8631	0	0	0	0.8031	110.9
2.55	0	0	0.8289	0	0	0	0.8204	108.58
2.56	0	0	0.7977	0	0	0	0.8354	106.42
2.57	0	0	0.7691	0	0	0	0.8483	104.4
2.58	0	0	0.743	0	0	0	0.8595	102.51

Appendix B

RF Link Budget Calculations

Global Variables	Variables	Units	Equations	Values
Frequency	f0	MHz		2400
Speed of Light	c	m/s		299792459
Wavelength	λ	M	λ/f0	0.124913525
Pi	π			3.141592654
Link Variables	**Variables**	**Units**	**Equations**	**Values**
Pa Power	Ppa	dBm		10
TX source	Ptx	dBm		10
TX connector Loss	LconTx	Db		-0.5
TX power	Pt	dBm	Pt=Ppa(C Loss)	9.5
Transmitter Antenna gain Tx	Gt	dBi		3
Effective isotropic radiated power	EIRP	dBm	EIRP=Gt*Pt	12.5
Distance	d	m		10
Free space loss	Lfs		Lfs=(λ/4πd)2	9.88096E-07
Free space loss in (dB)	Lfs	dB.		-60.05200803
Power at receiving antenna Rx	Prx	dB.	Prx=Lfs*EIRP	-47.55200803
Multipath Loss	Lmulti	dB.	N/A	
Receiver Antenna gain Rx	Gr	dBi		3
RX connector loss	LconRx	dB.	connetror loss	-0.5
RX Power, Free space path	Prfs	dBm.	Prfs=PrxGr(C Loss)	-45.05200803
Reciever sensitivity	**Variables**	**Units**	**Equations**	**Value**
RX Noise Figure	NF	dB.		4.8
Operating Temperature	To	K		290
Equivalent Noise Temperature	Te	K	Te=To(NF-1)	585.8
Boltzmann's constant	*k*	J/K		1.38E-23
Receiver Bandwidth	BWrx	MHz		10
Antenna Temperature	Tant	K		300
Noise Power (at RX)	Pn	dBm	Pn=K(Tant+Te)*BWrx	-9.91E+01
powre transfer formula			P(dBm)=10log(P(w))+30	
Signal to Noise Ratio	SNRrx	db.	SNRrx=Prx/Pn	5.41E+01

Appendix C

C.1 Conventional Optical Wireless with QAM Modulation Only

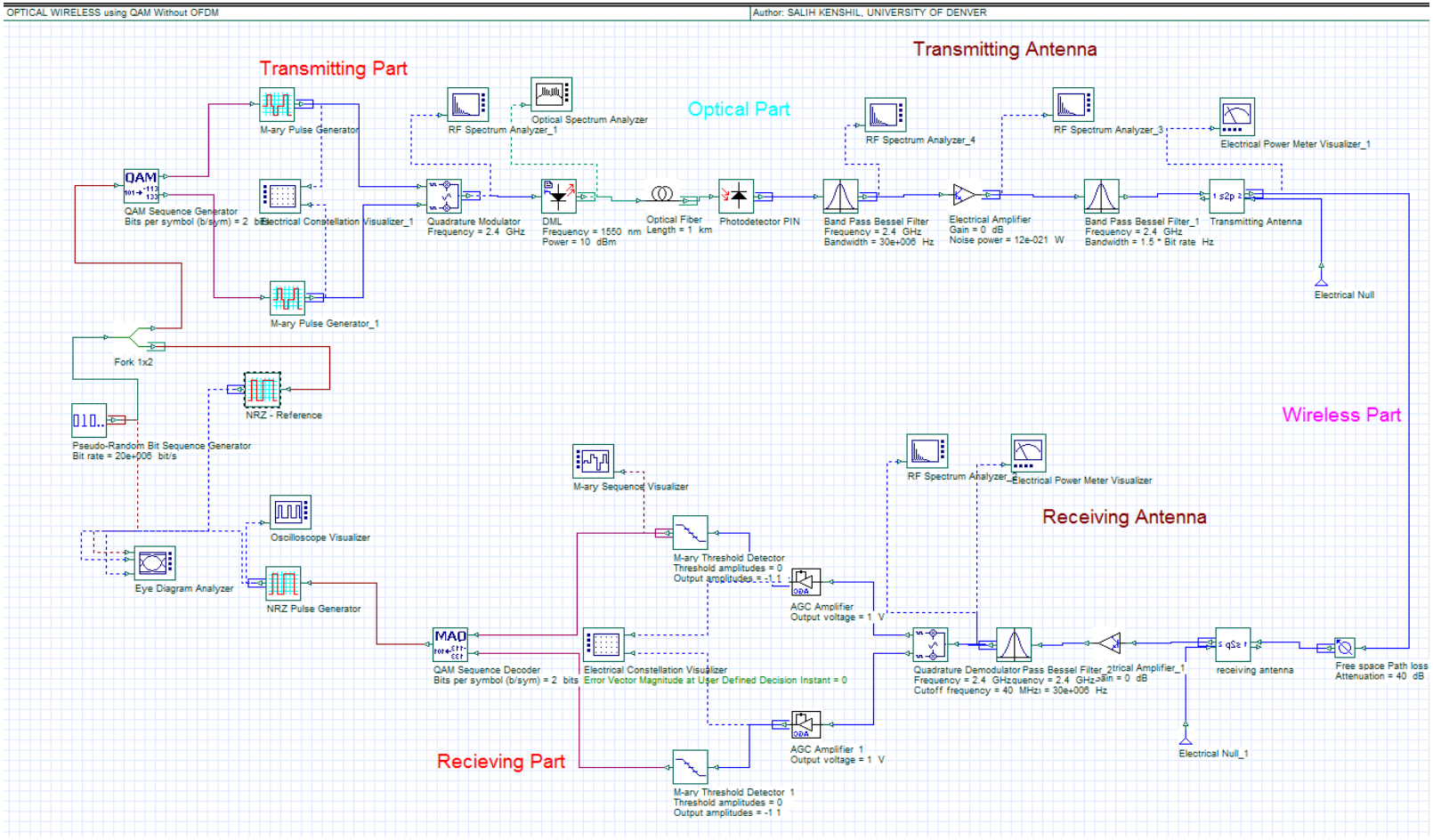

C.2 Optical OFDM Wireless System without External Modulator

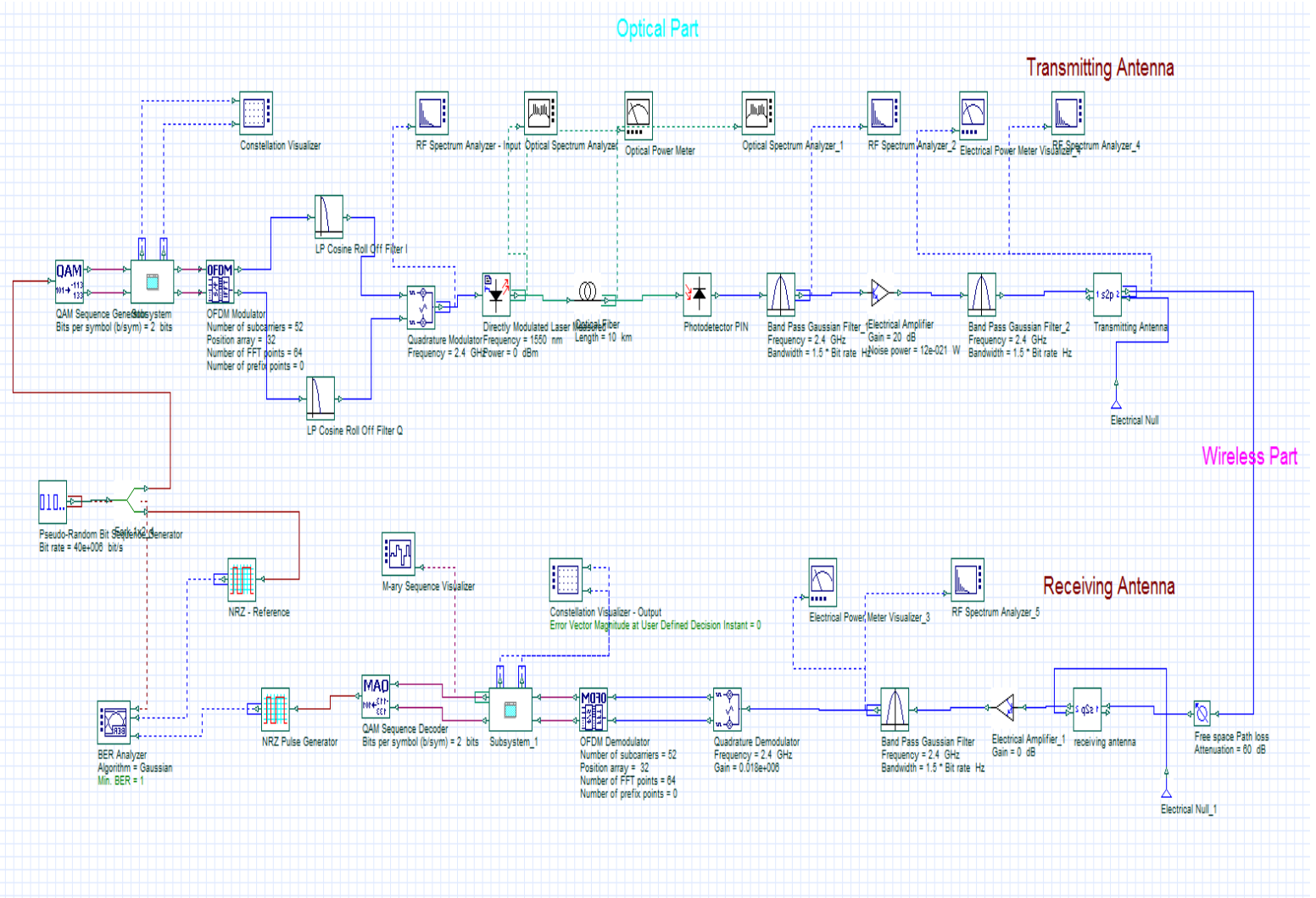

C.3 Optical OFDM Wireless System with External Modulator